NBSIR 82-2469

Effect of Ventilation on the Rates of Heat, Smoke, and Carbon Monoxide Production in A Typical Jail Cell Fire

NBSIR 82-2469

EFFECT OF VENTILATION ON THE RATES OF HEAT, SMOKE, AND CARBON MONOXIDE PRODUCTION IN A TYPICAL JAIL CELL FIRE

B. T. Lee

U.S. DEPARTMENT OF COMMERCE
National Bureau of Standards
National Engineering Laboratory
Center for Fire Research
Washington, DC 20234

March 1982

U.S. DEPARTMENT OF COMMERCE, Malcolm Baldrige, *Secretary*
NATIONAL BUREAU OF STANDARDS, Ernest Ambler, *Director*

TABLE OF CONTENTS

iii

LIST OF FIGURES

iv

LIST OF FIGURES (Continued)

Page

LIST OF TABLES

EFFECT OF VENTILATION ON THE RATES OF HEAT, SMOKE, AND CARBON MONOXIDE PRODUCTION IN A TYPICAL JAIL CELL FIRE

B. T. Lee

Center for Fire Research
National Bureau of Standards
Washington, DC 20234

Abstract

The rates of heat release and smoke development from a fire in a typical prison cell configuration were examined under four doorway ventilation conditions. Peak heat release rates varied from about 4500 kW for a 3.34 m^2 doorway opening down to 340 kW for a 0.17 m^2 opening. However, the total and rate of smoke generation were greater with the small opening. The peak carbon monoxide production rate varied from 0.03 kg/s for the large opening to 0.01 kg/s for the smallest opening. The quantity of carbon monoxide generated, however, was highest for the smallest opening with 5.3 kg produced over the fire duration of 1800 s. During the peak fire development in the configuration with the larger openings, temperatures inside the room reached about 1000°C with roughly two-thirds of the heat lost to the cell room boundaries. Peak thermal fluxes inside the room generally exceeded the ignition threshold value of about 20 kW/m^2 for clothing, bedding, and other light combustible fuel for all of the tests.

Key words: Fire growth; fuel load; heat release rate; prison cell fire; smoke

1. INTRODUCTION

1.1 Background

The National Institute of Justice has asked the National Bureau of Standards to prepare a fire safety evaluation system for prisons. One requirement of this system is an evaluation of the fire safety of multi-level prison cells located in a large, closed building. In the event of fire in such facilities, fans are used to purge the smoke and hot gases from the building. There is presently little, if any, information available on the heat release rate and production of smoke and combustion products from typical prison cell fires. Such information is needed to help establish the operational requirements for these fans. In addition, information is needed on the effect of ventilation on the prison cell fire development to aid in the design of more fire-safe cell rooms.

The heat release rate and production of smoke and combustion products depend on cell room construction and configuration; the type, quantity, and distribution of combustible materials in the cell; and, on the ventilation conditions. The latter depends on the size and location of the openings and on the location and capacity of any mechanical means of ventilating the cell. In practice, cell openings vary from small cell-door windows to barred, full wall openings.

The study presented here determined the rates of heat, smoke, and carbon monoxide production of one representative prison cell construction, configuration, and fire loading under four natural ventilation conditions. The fire load arrangement chosen for this study was based on a survey of some selected prison cells at the Maryland State Penitentiary. This survey indicated that each of the cells usually had one two-tier cot with cotton batting mattresses, wall-mounted shelves on the back wall, and one bookcase or bureau or storage cabinet located opposite the cots. Boxes of personal

2

belongings were often stored under the lower cot. Sheets, woven goods (such
as blankets and towels), and clothing were hung between the cots and wall
shelves and sometimes across the back wall. It is likely that fire initiat-
ing at either the bookcase or at the cots could spread along these combustible
materials to involve the entire cell.

1.2 Measurement of Heat Release Rate and Heat Losses

The rate of heat release is an important factor in determining the fire
hazard associated with combustible furnishings. There are two generally
recognized methods of measuring rate of heat release. One is the standard
textbook method of measuring the temperature rise of the combustion gases
and entrained air from the burning material. A problem with this technique
is heat loss to the measurement apparatus and to the surroundings. The
other method for measuring rate of heat release relies on a measurement of
the oxygen consumed in the fire. Both techniques for measuring rate of heat
were used here. In the method involving the measurement of oxygen consump-
tion, about 13 megajoules is obtained from each kilogram of oxygen consumed
in the burning of materials normally used in the construction and furnishing
of rooms [1][1]. Thus, the total rate of heat generation from burning furnish-
ings in a room can be obtained by measuring the oxygen content and volume
flow rate of the gases discharged from the fire. This total rate, $\dot{Q}_s$, in-
cludes the heat released from flames extending beyond the doorway, if this
occurs, as well as the heat produced inside the room. The portion of the
heat actually generated within the room by the burning furnishings, $\dot{Q}_d$, could
be calculated from the oxygen and flow measurements at the doorway opening.
Part of the heat produced in the room is lost to the room surfaces. This
heat loss can be obtained by first calculating $\dot{Q}_d$ and then subtracting away
h_d,   the flux of heat leaving the room at the doorway. The quantity h_d can
be calculated from measurements of the volumetric flow rate and the temperature

---

[1]Numbers in brackets refer to the literature references listed at the end of
 this report.

3

rise of the exhaust air at the doorway. The total flux of heat leaving the room fire, h_s, includes the heat release from flames extending beyond the doorway, in addition to the contribution from h_d. The quantity h_s can be based on the temperature rise of the mixture of combustion gases and entrained air at, e.g., the inlet of the exhaust collection hood, as was done in this study. The quantity h_s is equal to $\dot{Q}_s$ minus the heat loss to the room boundaries and the heat loss to the surroundings between the room doorway and the inlet of the exhaust collection system.

2. EXPERIMENTAL

2.1 Prison Cell Fire Tests

Figure 1 shows a general view of the test cell-exhaust hood arrangement. Interior dimensions of the compartment were 1.8-m wide, 2.7-m deep, and 2.4-m high. The back and two side walls were of concrete block construction. The ceiling was fabricated from two layers of 25-mm thick calcium silicate board supported along the rim of the block walls and attached to the under-side of several steel joists spanning the side walls. The front wall with the cell opening was constructed from a single layer of the calcium silicate board. Four fire tests, each having a different cell opening size, were conducted during this study. One of the tests had a small opening at the 1.37-m height and another small opening near the floor. The dimensions of these cell openings are shown in Table 1. The test cell was located adjacent to a large 3.66 x 4.88-m exhaust collector hood having an exhaust flow capacity of about 3 m^3/s.

4

2.2 Fire Load and Ignition Source

The fire load used for these tests was based on a survey of some
selected prison cells at the Maryland State Penitentiary. Figures 2 and **3**
show some actual cells which had estimated combustible fire loads of about
34 kg/m^2 of floor area. This compares with an average fire load of 23 kg/m^2 for
for a recreation room in a single family home in the Washington, DC metro-
politan area [2]. The total estimated mass of combustible material in a
cell room came to about 170 kg, with exposed clothing and miscellaneous
woven goods accounting for about 15 kg. Whenever possible, the room furnish-
ings observed were duplicated for the fire tests. Used cotton-batting
innerspring mattresses (having fire-retardant-treated tickings) were obtained
from a federal prison, and used clothing was purchased. Wool blankets,
which do not burn readily [3], were excluded in order to reduce costs, and
cardboard boxes of disposable paper files were used to replace the estimated
90 kg of loosely-filled combustible materials in storage cases or boxes,
Typical clothing fabric materials were also used to simulate some clothing,
towels, and other woven goods. Furnishings used in this study are listed in
Table 2. Each test used the same arrangement of the cots, shelves, and
bookcase as indicated in Figures 4 and 5. The two 0.76 x 1.94 m cots were
located 0.5 and 1.5 m from the floor. A 1.52-m wide, 0.46-m deep, and 0.66-m
high cabinet having two open shelves was mounted on the back wall 0.46 m down
from the ceiling. One wood bookcase, 1.52-m wide, 0.46-m deep, and 0.91-m
high, having two shelves, was positioned on the opposite wall of the cell
from the cots. The cover sheet at the head end of the upper cot was per-
mitted to drape down to the lower cot, and the cover sheet on the lower cot
was permitted to drape to the floor. Some of the clothes and fabric on the
top shelf of the bookcase were also permitted to drape over the paper files
on the lower shelf and to reach **down to the floor. In all** of the tests, the
fire was started with a match flame ignition of twelve pages of crumpled

newspaper located at the point indicated in Figure **4** where the bed sheet, extending down to the floor, contacted the clothes and fabric hanging from the bookcase.

2.3 Instrumentation

Location of all instrumentation in these cell room fire tests is indicated in Table **3** and Figure 4. Measurements of the vertical temperature profile halfway between the cots and the bookcase, and the total incident heat flux on the room surfaces were taken to characterize the thermal environment in the room. Thermal radiance was also measured at two positions on both sides of the cell opening, flush with the exterior wall, to examine the radiant heat transfer to adjacent cell rooms from flames emerging from the fire room. Temperatures, velocities, and oxygen and carbon dioxide concentrations in the exhaust gases at the opening were monitored for calculation of $\dot{Q}_d$, the rate of heat generation inside the room. The same measurements were made in the stack to determine $\dot{Q}_s$, the total rate of heat production by the fire. This total rate represented that heat produced inside the cell plus the portion of the heat released by the flames outside the opening. As mentioned in section 1.2, temperatures and velocities measured at the opening can also be used to determine h_d, the total flux of heat leaving the fire test room, i.e., the rate of heat release by the fire $\dot{Q}_d$, minus the heat losses to the room boundaries. An average temperature taken across the inlet of the exhaust collection hood was used to calculate the rate of heat release from individual items burning directly under the hood as well as to measure h_s, the total flux of heat from the fire test cell, including the heat from flames extending beyond the cell opening. Smoke was monitored in the stack, and carbon monoxide was also monitored in the stack and at the cell opening to help quantify these products of combustion from the cell room fires.

The average temperature at the inlet of the hood was monitored with a grid of *25* chromel-alumel thermocouples arranged in parallel. Each thermo-couple was made from Brown and Sharpe 24-gauge (0.51-mm or 0.020-in) diameter wire. Temperatures inside the room and at the cell opening were also measured with chromel-alumel thermocouples, made mostly with 0.51-mm wire. Due to the propensity of the large-size thermocouples for radiation error, thermocouples fabricated from 0.05-mm chrome1 and alumel wires were also employed at a sufficient number of locations to assure that the temperature readings were valid. Although the smaller wire thermocouples were more accurate, they were also more difficult to prepare and were more vulnerable to breakage. Heat flux was monitored with water-cooled total heat flux gauges of the Gardon type. Crumpled newspaper on top of the bookcase (0.91 m above the floor) was also used to indicate if and when the irradiance was sufficient to ignite such light combustible materials in the lower half of the room. Bidirectional velocity probes [4] were employed for measuring the air velocity in the cell doorway and to note the occurrence of any flow reversal along the doorway. The optical density of the smoke was determined by attenuation of a light beam in the stack. Neutral optical density filters were used to calibrate the light sensor over the range of optical densities from 0.04 to 3.0. The optical measurements, when calibrated in this manner, provide a useful measure of optical density. However, a more detailed calibration of the optical system with smoke of known concentration would be required for an accurate measurement of optical densities above about 1.5. Oxygen was sensed directly with a paramagnetic-type instrument at the stack and with chemical galvanic cells at the and cell opening. Non-dispersive infrared analyzers were used to record the concentrations of carbon monoxide and carbon dioxide at the stack and cell opening.

2.4   Corrections for Measurement of Heat Release Rate and Heat Outflow Rate

Diffusion-flame burner tests using propane were conducted inside the cell to calibrate the exhaust stack measurement of the rate of heat release

from room fires based on the oxygen depletion in the gases exhausted from the room. A heating rate of **485** kW was maintained for 300 **s**, and this was immediately followed with a rate of 1290 kW for another 300 **s.** The above calibration tests were then repeated with the burner positioned directly under the hood. In the calibration test, CO_2 was first removed ahead of the analyzer for the oxygen measurement. Then, the test was repeated with the CO_2 allowed to flow through the oxygen analyzer in order to evaluate the effect of CO_2 on such measurements. In the determination of heat release rates with and without the removal of CO_2, formulae given by Lawson et al **[5]** were employed. These formulae are given in appendix A.1.

When the burner was operated directly under the stack, and the CO_2 was removed, the values of the heat release rate calculated from oxygen consumption were 7 and 6 percent higher than those calculated from the actual low and high burner flow rates employed, respectively. In the test where the CO_2 was not removed, the values calculated from oxygen consumption were 6 and 7 percent higher, than the respective burner rates used. The flow rate, oxygen depletion, and carbon dioxide data used to calculate the heat release rates are shown at the end of appendix A.1. When the burner having the same heating rates was located inside the burn room, no significant.change occurred in the oxygen consumption measured in the stack, compared with having the burner under the stack. However, the mass flow through the stack based on measurements taken at a single location in the stack appeared to have increased by 25 percent, and this apparent increase was carried over to the calculation of the heat release rate. One plausible explanation for this apparent increase in **mass** flow **may be** that when the exhaust from the room entered the stack it clung to the inside surface closest to the room, resulting in highly non-uniform flow at the cross section of the duct where the measurement was taken. The heat release rate values calculated from the stack measurements were about 30 percent higher than those calculated from the actual low and high fuel flow rates used.

Heat release rate calculations based on the flow and oxygen depletion data at the doorway also averaged 30 percent higher than the actual burner rates employed. Much of this difference was due to the use of velocities taken at the vertical centerline of the doorway for calculating the mass flow from the fire room. Quintiere and McCaffrey [6] and Tu and Babrauskas [7] have found that calculations of mass based on outflow centerline velocities could be 20 to 30 percent greater than the actual flow.

Based on the above findings with the calibration burner, the heat release rates determined from measurements in the stack and cell opening for the fire tests have been multiplied by 0.77 to obtain the corrected values. The fact that both stack and doorway heat release rates need to be corrected by the same factor of 0.77 is a coincidence. Only the corrected heat release rates for $\dot{Q}_s$ and $\dot{Q}_d$, based on the stack and doorway measurements, respectively, are given in this report.

Accurate measurement of the rate of heat release based on the oxygen depletion of the exhaust in the stack or in the cell opening becomes difficult when small fuel items are burning, as small changes in oxygen concentration cannot be measured reliably with the instrumentation. Measurement of low heat release rates becomes more feasible when the burning item is directly under the hood where heat losses to the surroundings are small. Then the rate of heat release can be calculated from the temperature rise and mass flow of the combustion products and entrained air from the burning item. The temperature rise can be based on either the thermocouple in the stack or on the grid of 25 thermocouples at the inlet or neck of the hood. The thermo-couple grid gives a more accurate temperature measurement as it measures the average temperature over the stack opening and minimizes the thermal losses to the hood by measuring temperatures closer to the burning item. The ther-mocouple grid was then calibrated using propane as the fuel, with heating rates of about 19, 58, 118, 234, and 447 kW. The results shown in Figure 6 indicated that the temperature rise of the air as measured by the thermocouple

grid varied linearly with the rate of heat release from the calibration burner at about **4.66** kW/$^\circ$C rise in air temperature. This calibrated thermocouple grid was also used to provide a rough estimate of h_s, the total heat outflow rate from the cell fire tests. The heat outflow rate at the opening of the cell, h_d, can be calculated from temperatures and mass flow measurements taken at the cell opening. As with the cell room heat release rate measurements, the rates of heat outflow from the cell fire taken in the cell opening were also multiplied by the correction factor of 0.77. Only the corrected values for the rate of heat outflow, h_d, are given in this report.

2.5 Heat Release Rates of Individual Items

Individual items such as the mattress and bedding, bookcase, loose paper files, and piles of clothes and fabric materials were burned under the exhaust hood to provide a rough indication of their free-burning behavior, and thus provide some insight as to what to expect during the room fire tests with these materials, as well as to generate additional heat release rate data which could be used for predicting early room fire growth. The heat release rate for each item was determined from the rise in temperature in the calibrated thermocouple grid discussed in the preceding section. These were preliminary tests and were not intended to fully characterize the fire behavior of the individual items. **A** propane torch was used as the fire initiation source, and each item was ignited along one end. As a safety precaution, only **a** one-third section of the bookcase was burned directly under the hood to avoid potential damage to the hood and surroundings from a fire that could be too severe. The data from these tests are given in Figures 7 to 9.

3. RESULTS AND DISCUSSION

A summary of the heat release rate measurements for the four room fire tests is given in Tables **4** and 5 and in Figures 10 to 17. Table **4** also summarizes the methods used to calculate the rate of heat release and heat

outflow rate from the cell room fire tests. Figures 18 to 28 present tem-
perature profiles at various times, temperature histories at several locations
along the vertical centerline of the doorway, and the vertical distribution
of temperatures inside the test room. Table 6 gives the degree of fire
buildup, as indicated by the maximum temperature found in the doorway exhaust.
For each room fire, smoke production and the generation of CO in the fire
tests are also indicated in Table 6 and in Figures 29 to 34. Peak values of
thermal flux measured inside of the room and on the outside wall adjacent to
the doorway are shown in Table 7.

3.1 Heat Release

The rate of heat generation from the fire room was a strong function of
the ventilation conditions. The data from the exhaust stack in Table 4 shows
that the peak heat release rate increased from about 340 kW to over 4500 kW
as the doorway opening increased from 0.17 to 3.34 m^2. This would be expec-
ted for ventilation-controlled fires. Figure 35 shows that the peak heat
release rate increased linearly with the increasing doorway ventilation
parameter, $AH^{1/2}$, where A and H are the area and height of the doorway open-
ing, respectively. The parameter $AH^{1/2}$ is usually used for single openings.
However, since prison cell doors can have two separate openings, an effective
$AH^{1/2}$ must be used for this case. The effective value of $AH^{1/2}$ for test 2
with the two openings was derived by W. Parker in appendix A.2 and is shown
in Figure 35. The newspaper flashover indicator in tests 1, 3, and 4 ignited
at times of about 35, 45, and 100 s, respectively, with the likely attainment
of ventilation controlled conditions at the same times or shortly thereafter.
Test 2 appeared to have reached flashover or near flashover at about 780 s
with room air temperatures reaching about 600°C. Flashover is defined here
as the room condition where the thermal radiation level becomes high enough
to ignite light combustible materials, such as newspaper, in the lower half
of the room. This corresponds to the room fire condition where the thermal

11

radiation to the floor reaches about 20 kW/m^2 and the air temperatures reach 600 to 650°C near the ceiling and 500 to 550°C at the top of the doorway.

Table 4 and Figure 35 show that the differences between heat release rates measured in the stack and in the cell opening for the three fires with the largest openings were as great as 23 percent. With the small opening in test 2, there could have been considerable constriction or funneling of the flow out of the opening. This would have led to high centerline velocities which, when used to calculate mass flow, could have led to errors exceeding the 20 to 30 percent discussed in section 2.4. For test 2, the ratio of the calculated mass flow out of the cell room to that into the room was much higher than the ratios for the other three tests with the larger openings. This, in turn, led to a calculated rate of heat release at the cell opening for test 2 which was much too high. Consequently, the heat release rate measured in the cell opening for test 2 was 65 percent higher than that measured in the stack. For tests 1, 3, and 4 having the larger openings, the stack values were expected to be somewhat higher than the doorway values, since some of the fuel was being consumed outside of the room, as evidenced by flames extending beyond the doorway. Apparently, the measurement limitations may have masked any difference between the rates measured in the stack and cell opening. Figures 10 to 13 showed that the rates of heat release measured in the stack and cell opening agreed well over the duration of the fire. Averaged stack heat release rates over an 1800 s duration were **630,** 230, **690,** and 410 **kW,** corresponding to total heat release values of 1130, 410, 1240, and 740 MJ, for tests 1, 2, **3,** and 4, respectively. The lower average rate for test 4 may be due to a less severe room fire environment. This may be inferred from the temperature of the air exhausting through the opening (see Figures 21A, 22A, and 23A). The temperature in test 4 decreased to below 300 to 400°C much sooner than the doorway air temperatures for tests 1 and **3.**

The heat leaving the fire room is also given in Table 4 and Figures 14 to 17. Again, the stack values are close to the doorway values. Table 5 indicated that, on the average, only about one-third of the total heat released by the fire during the peak fire development was convected out through the doorway, with the remaining two-thirds of the heat lost to the room boundaries. In the prison cell tests discussed in section 2.4, with the calibration gas burner as the heat source, the heat outflow rate from the cell accounted for about one-half of the heat released by the burner. The flames from the burner extended across the ceiling to the doorway. No flames touched the back and sides of the room. In the fire tests of the jail furnishings, because of the distribution of fuel sources, the fire often contacted the walls as well as the ceiling. This could have resulted in a greater relative heat loss to the walls of the room itself. In addition, the furnishing fires produce less transparent flames than propane fires, implying greater flame radiation, with subsequent larger heat loss to the cell surfaces.

3.2 Room Air Temperatures

The air temperature in the upper part of the room is a good measure of fire buildup [8]. Temperatures measured with the vertical thermocouple tree inside the room can give a good but often approximate measure of the temperature environment in the upper part of the room. Local heating and flame contact can give readings that are higher than average. The hot air inside the room usually becomes well mixed by the time it is exhausted through the doorway. Consequently, the peak doorway air temperature may be a more reliable indicator of the fire buildup than the interior air temperature measurement. Peak doorway air temperatures given in Table 6 varied from $867^{\circ}C$ at 2110 s for test 2 to $1079^{\circ}C$ at 380 s for test 3. While test 2 with a very small opening of 0.17 m^2 took over 2000 s to reach its peak doorway temperature, the other tests with doorway openings greater than 1.0 m^2 took only about 500 s or less to reach the peak fire buildup.

Analysis of the vertical temperature profiles in the doorway (Figures 18 to 20) and the temperature histories at the doorway (Figures 21 to 24) revealed that the monitoring of air temperatures with large junction thermocouples could lead to errors. When there was considerable thermal stratification, as in the doorway, the large junction thermocouples in the hot upper zones behaved as thermal sources radiating to the outside and to the cooler lower levels. The large size thermocouples in the cooler lower part of the doorway acted as heat sinks for the radiation from the hot air, smoke, and heated surfaces in the upper part of the room. Consequently, large junction thermocouples registered temperatures which were too low in the hot zone and **too** high in the cooler zone. Small junction thermocouples are less prone to radiation errors, **as** the convective heat transfer component overwhelms the radiative heat transfer component when smaller size junctions are used. The differences due to thermocouple size were particularly noticeable in Figures 18A and 19A where errors of as much as 90, 230, and $100^{\circ}C$ were observed near the top, middle, and bottom part of the doorway opening. Consequently, only the data with the small junction thermocouples were used for the mass flow and heat release rate calculations at the doorway.

When the space is completely filled with flames and little thermal stratification exists, large and small junction thermocouples indicate about the same temperatures. This can be seen in the interior air temperature histories in the upper part of the cell, shown in Figures 25 to 28, at times following flashover.

3.3   Production of Smoke and Carbon Monoxide

The smoke production in the prison cell fire tests can be expressed by the extinction cross section generated. This extinction cross section, $E(m^2)$, is equal to the total mass of the smoke generated, $M_T(kg)$, times the specific extinction coefficient, $K(m^2/kg)$. The relationship between E and the optical density, O.D., is given below. The optical density is defined as

14

$$\text{O.D.} = \log_{10} \frac{100}{T} = \log_{10} e^{KML} = 0.434 \text{ KML} \tag{1}$$

where T is the percent transmission of the smoke meter, L(m) is its path length, and M(kg/m^3) is the mass concentration of the smoke. Thus, E is given by

$$E = KMV = 2.3 \text{ V} \quad \underline{\qquad} \tag{2}$$

where V(m^3) is the volume of the smoke produced. Since V(m^3/s), the volume flow rate of the air through the doorway, and the quantity O.D./L change during the test, E is determined by integrating over the duration of the test, or

$$E = 2.3 \int_{o}^{t} \dot{V} \left(\frac{\text{O.D.}}{L}\right) dt \tag{3}$$

Equation (3) can also be related to measurements performed in the ASTM E 662 test with the smoke density chamber [9]. The quantity E is equivalent to the product of the specific optical density measured in that test and the specimen surface area employed in the test. Equation (2) can be used to estimate the average O.D. per meter beyond the room of fire origin if the smoke is dispersed over a volume V, and the effect of smoke deposition and coagulation is neglected.

If the total mass of smoke generated were also measured routinely during some future room fire tests, then the average specific extinction coefficient K could be determined (i.e., K = E/M$_T$). Since K is a property of the smoke rather than a measure of its quantity, some insight might be gained into the nature of the smoke. This might help relate O.D. to visibility and provide an indication of its coagulation properties, since K is a function of par-ticle diameter. If a functional dependence of K can be established for room

fires, it may be possible to utilize data on mass generation rates of smoke from material tests to predict the optical density.

Peak smoke concentrations given in Table 6 showed that test *3* with the **3.34** m^2 doorway opening and test 4 with the 2.23 m^2 opening had peak O.D./L values of 1.12 and 1.25 m^{-1}, respectively. These concentrations correspond to extinction cross section per unit time values of 16.7 and 19.6 m^2/s, respectively. In contrast, test 2 had the smallest opening at 0.17 m^2 and experienced the lowest level of fire buildup, but generated the most smoke with an **O.D./L** greater than 2.5 m^{-1}, corresponding to an extinction cross section per unit time value of greater than 24.7 m^2/s. Values of O.D./L above 2.5 m^{-1} are not very meaningful as this is the upper limit of the instrumentation. Smoke generation histories for fire tests 2, 3, and 4 are given in Figure 29. The light sensor used to measure smoke in test 3 mal-functioned at about 120 s; however, visual observation indicated that the most heavy smoke production occurred prior to that time. No smoke data were recorded for test 1 due to malfunctioning of the instrument. Equation *(3)* was used to calculate the smoke production as a function of time from cell fire tests 2 and 4, with the results shown in Figure 30. Calculation of the extinction coefficient for test 2 in Figure 30 assumed that the peak O.D./L value did not exceed *2.5* m^{-1}. This meant that the actual smoke production was higher than that shown for test 2. Thus, the data in Figure 30 show that over a duration of 1800 s, the fire in the cell with the small opening pro-duced at least *30* percent more smoke than the fire in the cell having a large opening.

Peak concentrations of CO and the times at which they oc   in the stack and at 0.30 m down from the top of the cell opening are give   , Table 6 for the four prison cell fire tests. Concentration levels of CO   this cell opening location ranged from 3.5 percent for test 1 to 8.2 p   t for test 2. Stack concentrations of CO were an order of magnitude   to the dilution of the exhaust with entrained air. A more meanin   nting of

16

CO is in terms of mass flow, based on the measurement of the mass flow rate of the combustion gases and entrained air from the cell fire and on the measurement of the CO concentration of this gas-air mixture, Figures 31-34 show the mass flow histories for CO for the room fire tests. Differences between the doorway and stack measurements of the peak mass flow rate of carbon monoxide exceeded the differences between the peak rates of heat release taken at the same two locations for tests 1, 3 and 4. The reason for these larger differences can be attributed to oxidation of the CO exhausting from the doorway. Analysis of the ratio of CO to CO_2 showed that this ratio was much lower in the stack than at the doorway during the peak fire development. The maximum mass flow of CO at the cell opening ranged from 0.017 kg/s for test 2 to 0.064 kg/s for test 3. The peak mass flow at the stack varied from 0.010 kg/s for test 2 to 0.033 kg/s for test 4, Test 2, however, produced the highest quantity of CO. The production of CO, as measured in the stack, was 3.7, 5.3, 3.9 and 4.9 kg for cell fires 1, 2, 3, and 4, respectively, over the test period of 1800 s.

3.4   Thermal Flux and Radiation

Peak thermal flux measurements inside the room and on the outside wall close to the doorway are reported in Table 7. The highest flux values were recorded for test 3 'with the largest doorway opening, and the lowest values were found for test 2 having the smallest opening. The maximum flux values for the ceiling and walls in the upper part of the room ranged from 22.6 to 121.8 kW/m^2 for the cell room tests. Peak radiative fluxes to the floor in tests 1, 3, and 4 exceeded 47 kW/m^2, a value larger than the 20 kW/m^2 chosen to represent threshold ignition conditions [10]. Test 2, however, had a peak recorded flux of only 8.8 kW/m^2 at the center of the floor. Test 2 did develop interior and doorway temperatures of over 800°C, which indicated that flashover conditions were achieved. Fallen material from the bunks and bureau could have been partially shielding the flux meter from the radiation from the upper portion of the room.

17

At a height of 1.5 m along the exterior wall and 1.8 m away from the doorway, peak flux levels of **2.0** to **9.1** kW/m^2 were measured for tests 1, 3, and **4.** The flux meter at that location was not functioning properly during test 2. At the same height along the outside wall, but 0.2 m away from the other side of the opening, peak values of **19.3** to 23.8 kW/m^2 were recorded in tests 1, **3,** and **4.** These flux levels were reached as early as **40 s,** as in test **3,** and were sufficiently high to result in the ignition of some adjacent fuels had they been present. For test 2, exhaust from the fire room was primarily hot air and smoke, with a brief period at about **900 s** where a little extension of the flames occurred beyond the doorway opening. The plume from the opening in test 2 was relatively small due to the restricted size of the opening. Consequently, the peak thermal radiation from this plume reached only about 0.7 kW/m^2 at the wall location 0.2 m away from the doorway.

4. SUMMARY

The total rates of heat, smoke, and carbon monoxide production were measured during four fire tests in a 1.8-m by 2.7-m by 2.4-m high jail cell having similar fire loads of **34** kg/m^2 and a range of ventilation conditions. The findings from this series of tests are given below. No additional tests were performed to assess the repeatability of these results. However, in another study of fully furnished room fires [11], good repeatability was found between tests for measurements of interior temperatures, thermal fluxes, and times to reach room flashover.

1. In those prison cell fire tests where the cell door openings were 1.1 m^2 or greater and where a combustible fire load of 34 kg per m^2 of floor area was employed, flashover occurred between 30 and 100 **s.** Peak heat release rates between 1460 and 4510 kW occurred at times from 80 to **396 s.** Total heat generation ranged from **740** to 1240 **MJ** for a fire duration of 1800 **s.** Maximum temperatures of the air discharging from the cell reached about 1000°C.

2. With **a** doorway opening of 0.17 m^2 and the same fire load of 34 kg/m^2, flashover or near-flashover with accompanying interior temperatures of about 600°C occurred at 780 **s**. The peak heat release rate of about 340 kW did not occur until about 700 *s*. Peak temperature of the exhaust from the room reached 867°C at 2110 s. However, the reduction of ventilation due to the small opening resulted in a higher peak rate of smoke generation and at least 30 percent more total smoke than that produced from a room fire with a larger opening.

3. On the average, at the time of peak rate of heat release from the fire, roughly two-thirds of the heat was lost to the cell room walls, ceiling, and floor, with only one-third convected away through the doorway.

4. Carbon monoxide reached peak levels of 0.013, 0.033, and 0.028 kg/s in the exhaust collection hood at times between 90 and 110 s for cell openings of 1.11, 2.23, and 3.34 m^2, respectively. **A** maximum level of 0.010 kg/s was attained at 680 s in test 2 with the small opening. Total generation of carbon monoxide, over the test duration of 1800 **s**, was highest for the small opening with 5.3 kg produced as compared with 3.7, 4.9, and 3.9 kg for cell openings of 1.11, 2.23, and 3.34 m^2, respectively.

5. Peak heat fluxes inside the room generally exceeded the 20 kW/m^2 value which is an approximate threshold value for ignition of light combustible fuel such as cotton bed sheets and upholstery fabrics. Maximum fluxes at a height of 1.5 m on the outside wall reached about 20 kW/m^2 at about 0.2 m from one side of the opening and dropped rapidly with increasing distance from the doorway.

6. The cell fire having the small opening resulted in a lower
heat release rate, less total heat production, and lower air
temperatures than the fires having the larger openings.
However, total smoke generation and the total production of
carbon monoxide were greater with the small opening.

5. ACKNOWLEDGMENTS

6. REFERENCES

[1] Huggett, C., Estimation of Rate of Heat Release by Means of Oxygen Con-
sumption Measurements, Fire and Materials, 4, 61-65, 1980.

[2] Fang, J. B., Fire Performance of Selected Residential Floor Constructions
Under Room Burnout Conditions, NBSIR 80-2134, December 1980.

[3] Lee, B. T. and Parker, W. J., Naval Shipboard Fire Risk Criteria--
Berthing Compartment Fire Study and Fire Performance Guidelines,
NBSIR 76-1052, September 1976.

[4] McCaffrey, B. J. and Heskestad, G., A Robust Bidirectional Low-Velocity
Probe for Flame and Fire Application, Combustion and Flame, 26, 125-127
(1976).

[5] Lawson, J. R. et al, Development of an Oxygen Consumption Calorimeter,
NBSIR in preparation.

[6] Quintiere, J. and McCaffrey, B., The Burning of Wood and Plastic Cribs
in an Enclosure, Vol. I, NBSIR 80-2054, November 1980.

[7] Tu, K. M. and Babrauskas, V., The Calibration of a Burn Room for Fire Tests on Furnishings, NBS Technical Note 981, December 1978.

[8] Parker, W. J. and Lee, B. T., A Small-Scale Enclosure for Characterizing the Fire Buildup Potential of a Room, NBSIR 75-710, June 1975.

[9] Standard Test Method for Smoke Generated by Solid Materials, ASTM E 662.

[10] Fang, J. B., Fire Buildup in a Room and the Role of Interior Finish Materials, NBS Technical Note 879, June 1975.

[11] Fang, J. B., Repeatability of Large-Scale Room Fire Tests, Fire Technology, Vol. 17, No. 1 (February 1981), pp. 5-16.

Table 1. Doorway dimensions and test conditions in prison cell fire tests

Test	Doorway Opening Dimensions				Ambient Room Conditions	
	Height H (m)	Width W (m)	Area A (m^2)	$AH^{1/2}$ ($m^{5/2}$)	Temp. (^oC)	Relative Humidity %
1	1.83	0.61	1.11	1.50	26	49
2	*	*	0.17	0.30*	17	49
3	1.83	1.83	3.34	4.52	19	45
4	1.83	1.22	2.23	3.02	20	42

* A 0.305m x 0.305m opening in the door, with the lower ledge at a height of 1.37m, and a 0.102m high by 0.711m wide opening along the bottom of the door. The effective value of $AH^{1/2}$ was derived by Parker in appendix A.2.

Table **2.** Fuel loading in prison cell fire tests

Fuel Item	Combustible Weight in Kilograms			
	Test 1	Test 2	Test 3	Test 4
2 mattresses*	27.7	26.3	27.2	31.8
Bedding (2 pillows, 2 pillow cases, 4 sheets)	4.5	4.5	4.5	4.5
Loose paper files and cardboard boxes of paper files **	90.8	90.8	90.8	90.8
Plywood bookcase	42.7	29.1	30.4	30.0
Clothes †	9.1	9.1	9.1	9.1
Fabric ††	5.4	5.4	5.4	5.4
Total Combustible Fuel	180.2	165.2	167.4	171.6

* Mattress weight excluding weight of innersprings.
** 45.4 kg of loose files in lower shelf of bookcase, three 9.1-kg boxes
   of files under bed, and two 9.1-kg boxes of files in lower shelf of
   wall cabinet.
† Consisted of 4 jackets, 10 pants and 10 shirts for a total of 9.1 kg.
   1.8 kg of clothing in wall shelves, 5.4 kg in upper shelf of bookcase, and
   1.8 kg suspended on wires in front of wall shelves and along the wall over
   the bookcase.
†† 0.9 kg of fabric in upper wall shelves, 1.8 kg crumpled up in upper shelf
   of bookcase, 1.4 kg hanging on wires in front of wall shelves, and another
   1.4 kg used for privacy curtains hanging on wires alongside the cots.
   80 percent of material was 0.12 kg/m^2 fabric having a fiber blend of
   65% polyester - 35% cotton, while 20 percent of the material was 0.24 kg/m^2
   fabric with a blend of 65% polyester - 35% rayon.

Table 3. Location of instrumentation

Type of Transducer	Location
1 smoke meter	Exhaust hood
1 gas sample port (O_2, CO, CO_2)	Exhaust hood
1 velocity probe	Exhaust hood
1 0.51-mm thermocouple	Exhaust hood
25 0.51-mm thermocouples	Inlet area of exhaust hood
12 0.51-mm thermocouples	Following distances below the center of the ceiling (m): *O*, 0.025, 0.10, 0.30, 0.60, 0.90, 1.20, 1.50, 1.80, 2.10, 2.34, 2.44
5 0.05-mm thermocouples	Following distances below the center of the ceiling (m): 0.10, 0.60, 1.20, 1.80, 2.34
7 flux meters	Center of ceiling and center of floor. 0.30 and 0.76 m below ceiling on cot side of wall and 0.76 m below ceiling on bookcase side. 1.5 m above floor level on exterior wall, 2.1 m to left of right edge of doorway and 0.2 m to right of right edge of doorway.
11 0.51-mm thermocouples	Following distances below the top of the doorway (m): 0.025, 0.10, 0.30, 0.50, 0.70, 0.90, 1.10, 1.30, 1.50, 1.70, 1.83
5 0.05-mm thermocouples	Following distances below the top of the doorway (m): 0.10, 0.50, 0.90, 1.30, 1.70
3 gas sample ports (O_2, CO, CO_2)	Following distance below the top of the doorway (m): 0.30, 0.70, 1.10
5 bi-directional velocity probes	Following distance below the top of the doorway (m): 0.10, 0.50, 0.90, 1.30, 1.70

Table 4   Heat and mass data measurements

Test	Doorway Opening (m²)	Stack Peak Heat Release Rate $\dot{Q}_s$ (kW)	Time to $\dot{Q}_s$ (s)	Flux of Heat from Cell (Measured in Stack), h_s, at Time of $\dot{Q}_s$ (kW)	Doorway Peak Heat Release $\dot{Q}_d$ (kW)	Time to $\dot{Q}_d$ (s)	Flux of Heat from Cell (Measured in Cell Opening), h_d, at Time of $\dot{Q}_d$ (kW)
1	1.11	1460	396	500	1460	552	640
2	0.17	340	690	90	560	770	--
3	3.34	4510	80	1380	3840	110	1310
4	2.23	3100	80	890	3500	100	860

Notes:

1. $\dot{Q}_s$ is the heat release rate of the burning contents inside the cell; it includes the heat released from flames extending beyond the cell opening. $\dot{Q}_s$ is based on oxygen depletion and mass flow measurements in the stack.

2. $\dot{Q}_d$ is the heat release rate of the burning contents inside the cell; it is based on oxygen depletion and mass flow measurements at the cell opening.

3. h_s is the rate of heat convected from the cell fire; it is based on the calibration factor of 4.66 kW per °C rise in the stack thermocouple grid.

4. h_d is the heat convected through the cell opening; it is calculated from the mass flow and temperature rise of the air discharging at the cell opening.

5. $\dot{Q}_s$, $\dot{Q}_d$, and h_d have been multiplied by the 0.77 correction factor discussed in section 2.4. Corrected values given in above table.

Table 5. Fraction of heat release convected away from fire room
at time of peak heat release rate

Test	Stack Flux of Heat ÷ Stack Peak Heat Release Rate $h_s/\dot{Q}_s$	Doorway Flux of Heat ÷ Doorway Peak Heat Release Rate $h_d/\dot{Q}_d$
1	0.34	**0.44**
2	0.26	--
3	0.31	0.34
4	0.29	0.25
	0.30 Average	0.34 Average

Note: $\dot{Q}_s$, h_s, $\dot{Q}_d$, and h_d are defined in Table 4.

26

Table 6. Other doorway and exhaust hood measurements

Test	Doorway Opening (m²)	Peak Doorway Temp. T1 (°C)	Time to T1 (s)	Peak CO in Stack Conc. (%)	Time (s)	Peak CO, 0.30 m Down From Doorway Conc. (%)	Time (s)
1	1.11	1007	514	0.35	102	3.5	114
2	0.17	847	2110	0.23	640	8.2	670
3	3.34	1079*	380	0.58	100	5.0	100
4	2.23	939	140	0.46	90	5.7	80

Test	Doorway Opening (m²)	Peak smoke in stack Conc. (O.D./m)	Time (s)	Volumetric Flow (m³/s)	Extinction Cross Section per Unit Time (m²/s)
1	1.11	--	--	--	--
2	0.17	>2.5	700	4.3	>24.7
3	3.34	1.42	80	3.5	13.7
4	2.23	1.25	40	3.8	13.3

*For test 3, the peak value occurred at 0.50 m from top of doorway. In tests 1, 2, and 4 peak temperatures occurred at 0.10 m from top of doorway.

Table 7. Thermal flux measurements

Location	Test 1 Peak Flux (kW/m^2)	Test 1 Time (s)	Test 2 Peak Flux (kW/m^2)	Test 2 Time (s)	Test 3 Peak Flux (kW/m^2)	Test 3 Time (s)	Test 4 Peak Flux (kW/m^2)	Test 4 Time (s)
Center of ceiling	47.8	426	36.5	70	106.0	90	73.0	60
Center of floor	67.3	78	8.8	300	96	80	47.7	70
0.30 m below ceiling on end side of wall	38.3	30	33.3	70	81.9	90	37.8	30
0.76 m below ceiling on end side of wall	30.7	450	22.4	1980	43.3	100	32.8	60
0.76 m below ceiling on bookcase side of wall	51.8	420	33.1	470	121.8	70	34.6	30
1.5 m above floor level, 2.1 m on exterior wall, to left of right edge of doorway	2.0	516	*	*	9.1	60	3.6	40
1.5 m above floor level, 0.2 m on exterior wall, to right of right edge of doorway	19.3	54	0.4	630	23.8	40	19.7	210

* Data unavailable

TOP VIEW

EXHAUST HOOD

3.66m

4.88m

CELL ROOM

2.7m

1.8m

N

SIDE VIEW

CONCRETE FLOOR

1.2m

EXHAUST HOOD

SKIRT

CELL ROOM

2.4m
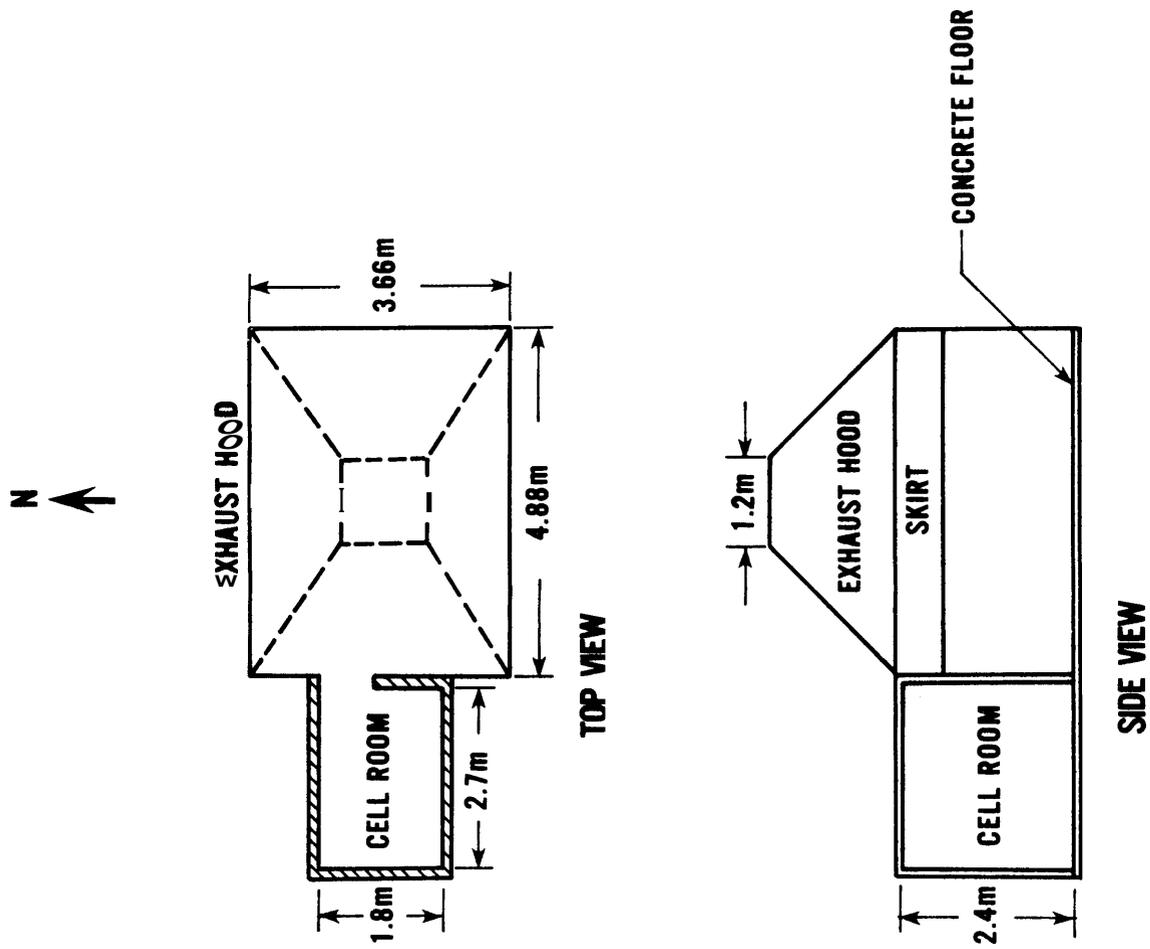
Figure 1. General view of test cell-exhaust ho a c mpl x

Figure 2. **Representative prison cell arrangement**

Figure 3. Representative prison cell arrangement

Scale:
|← 1m →|

SHELVES

~~SHELVES~~

⑤

④

③
②

BOOK-CASE

⑥

IGNITION
LOCATION ⟍
⊗

①

⑦

⑧
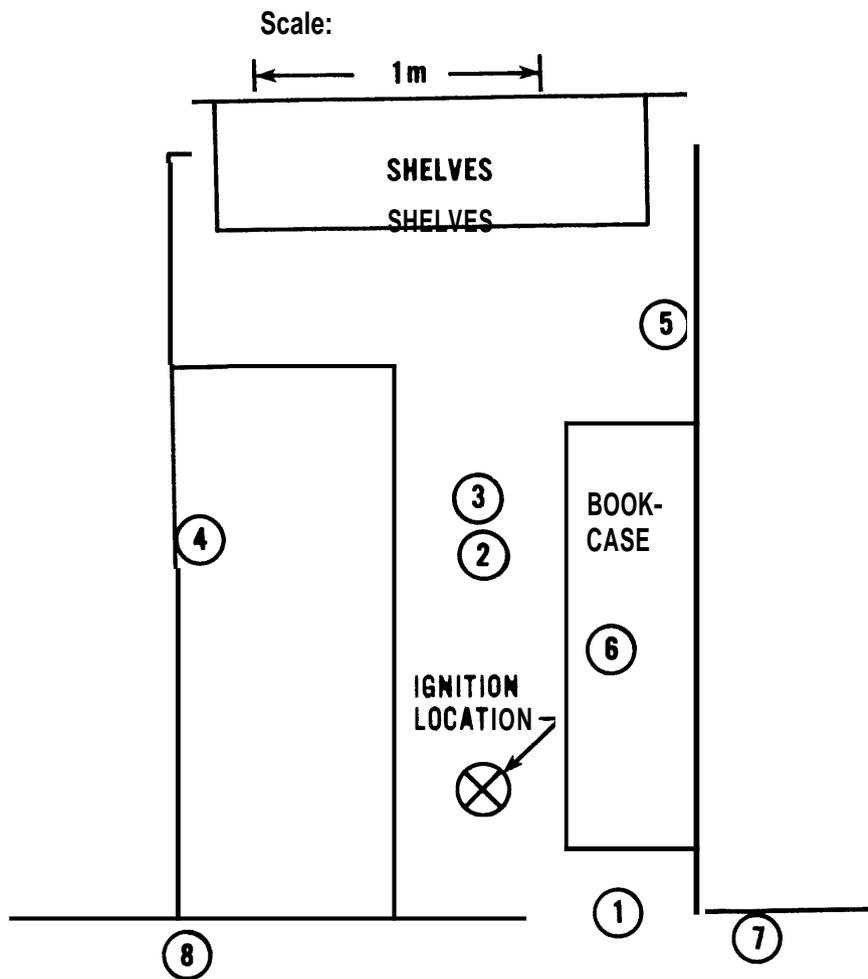
LOCATION   **INSTRUMENTATION**

1 —— DOORWAY THERMOCOUPLE TREE, VELOCITY PROBES, GAS SAMPLE PORTS

2 —— ROOM THERMOCOUPLE TREE

3 —— FLOOR AND CEILING FLUX METERS

4,5 —— WALL FLUX METERS

6 —— NEWSPRINT FLASHOVER INDICATOR

7,8 —— FLUXMETERS FLUSH WITH EXTERIOR WALL AND FACING AWAY FROM THE CELL

Figure 4. Plan view of fire test cell room arrangement

32

Figure 5. Test cell fuel arrangement
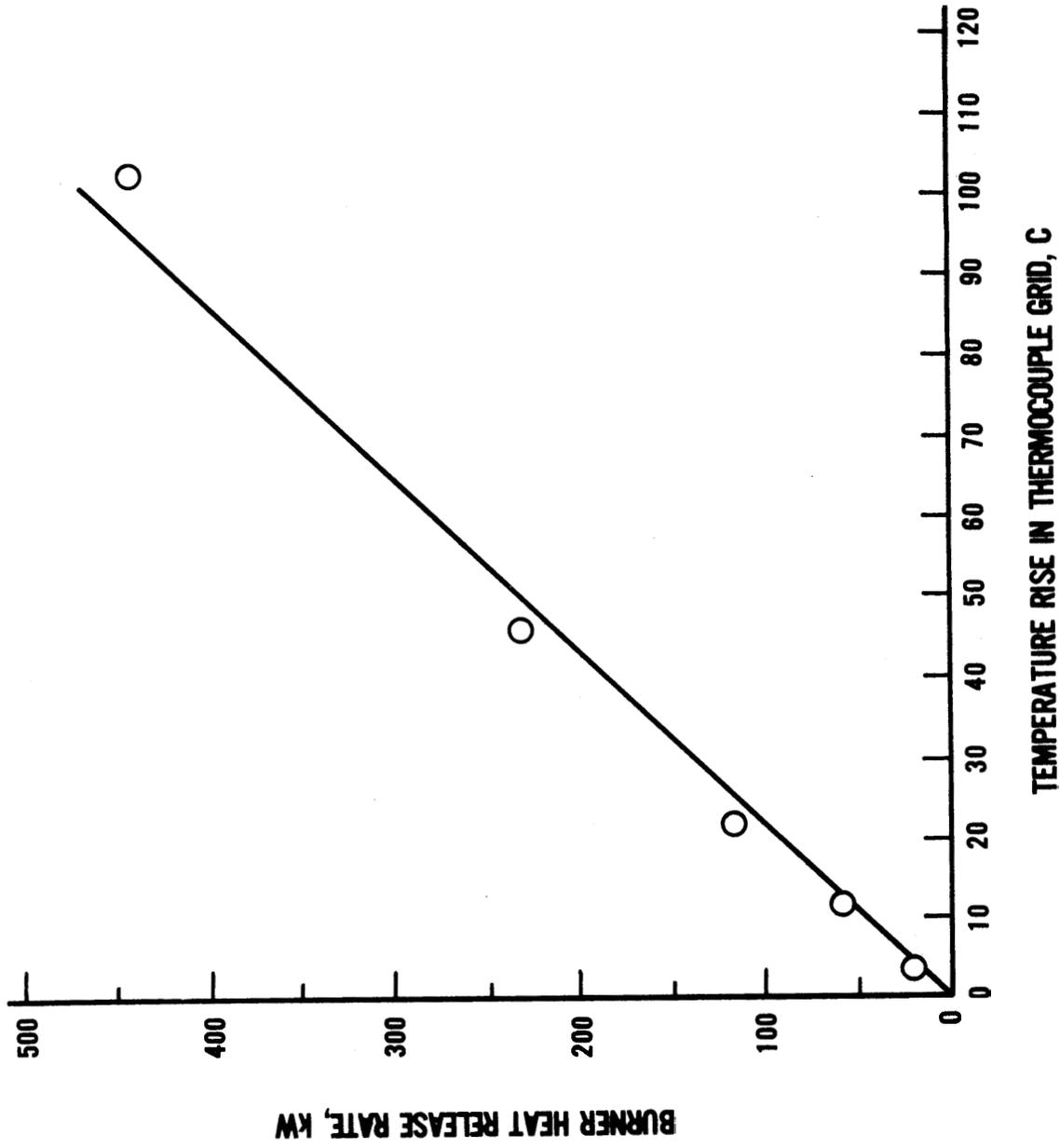
Figure 6. Heating rate versus temperature rise in the TC grid.

FULL SIZE 32kg MATTRESS, 0.9kg PILLOW, 2 SHEETS.
TORCH IGNITION IN ONE CORNER OF MATTRESS NEAR PILLOW.

10kg SECTION OF PLYWOOD BOOKCASE. TORCH IGNITION
AT LOWER INSIDE CORNER.

9.1kg CARDBOARD BOX OF FILES. TORCH IGNITION ALONG
ONE VERTICAL CORNER.

HEAT RELEASE RATE, kW

TIME FROM IGNITION, Min
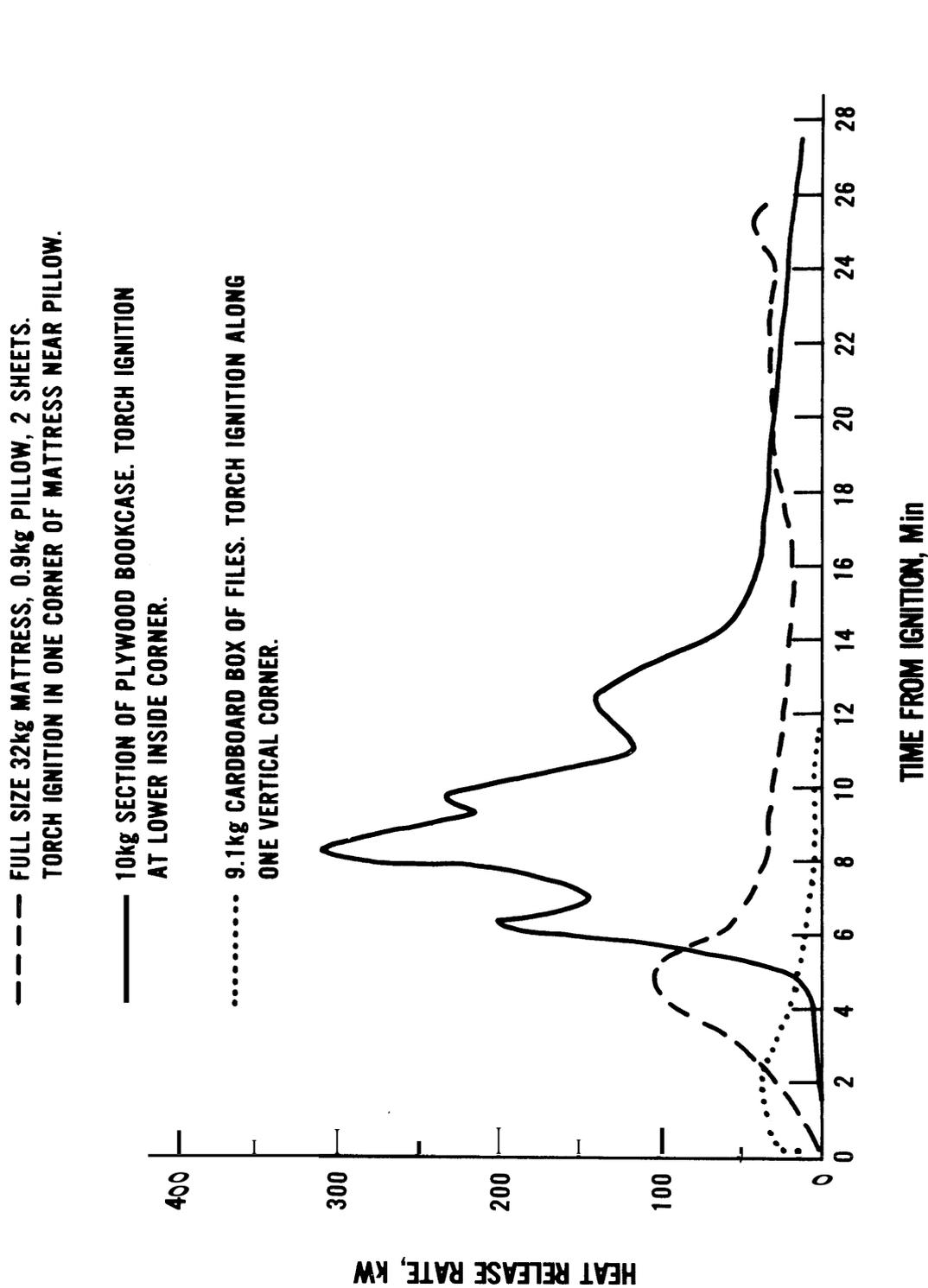
Figure 7.   Heat release histories for mattress with box of paper files

35
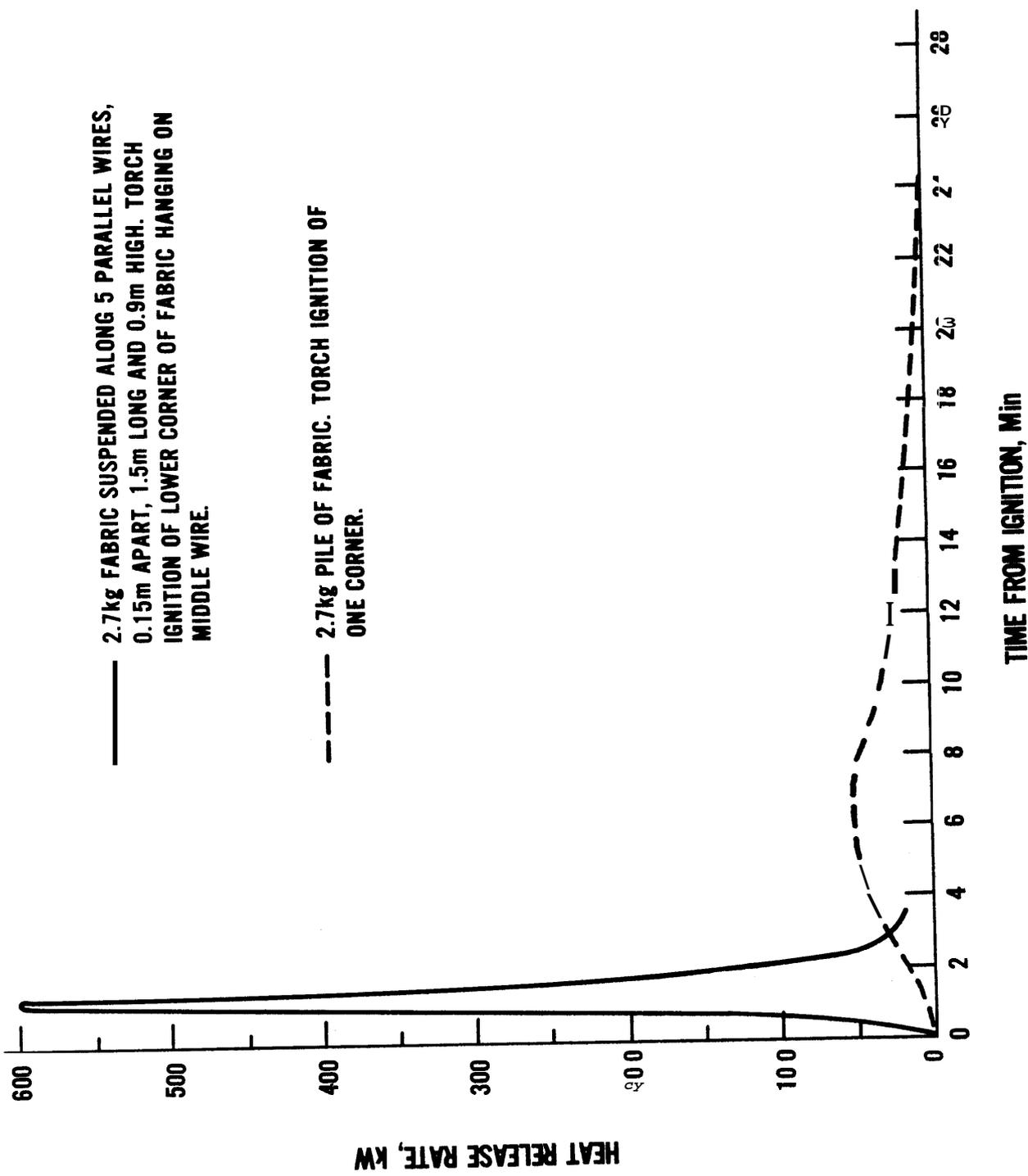
Figure 8. Heat release history for fabric material

2.7kg FABRIC SUSPENDED ALONG 5 PARALLEL WIRES, 0.15m APART, 1.5m LONG AND 0.9m HIGH. TORCH IGNITION OF LOWER CORNER OF FABRIC HANGING ON MIDDLE WIRE.

2.7kg PILE OF FABRIC. TORCH IGNITION OF ONE CORNER.

HEAT RELEASE RATE, kW

TIME FROM IGNITION, Min

4.5kg CLOTHES (2 JACKETS, 5 PANTS, 5 SHIRTS) SUSPENDED ALONG 3 PARALLEL WIRES, 0.15m APART, 1.5m LONG AND 0.9m HIGH. TORCH IGNITION OF LOWER CORNER OF CLOTHES HANGING ON MIDDLE WIRE.

------ 4.5kg PILE OF SAME CLOTHES. TORCH IGNITION ALONG ONE CORNER.

HEAT RELEASE RATE, kW

TIME FROM IGNITION, Min

Figure 9. Heat release history for clothes

37
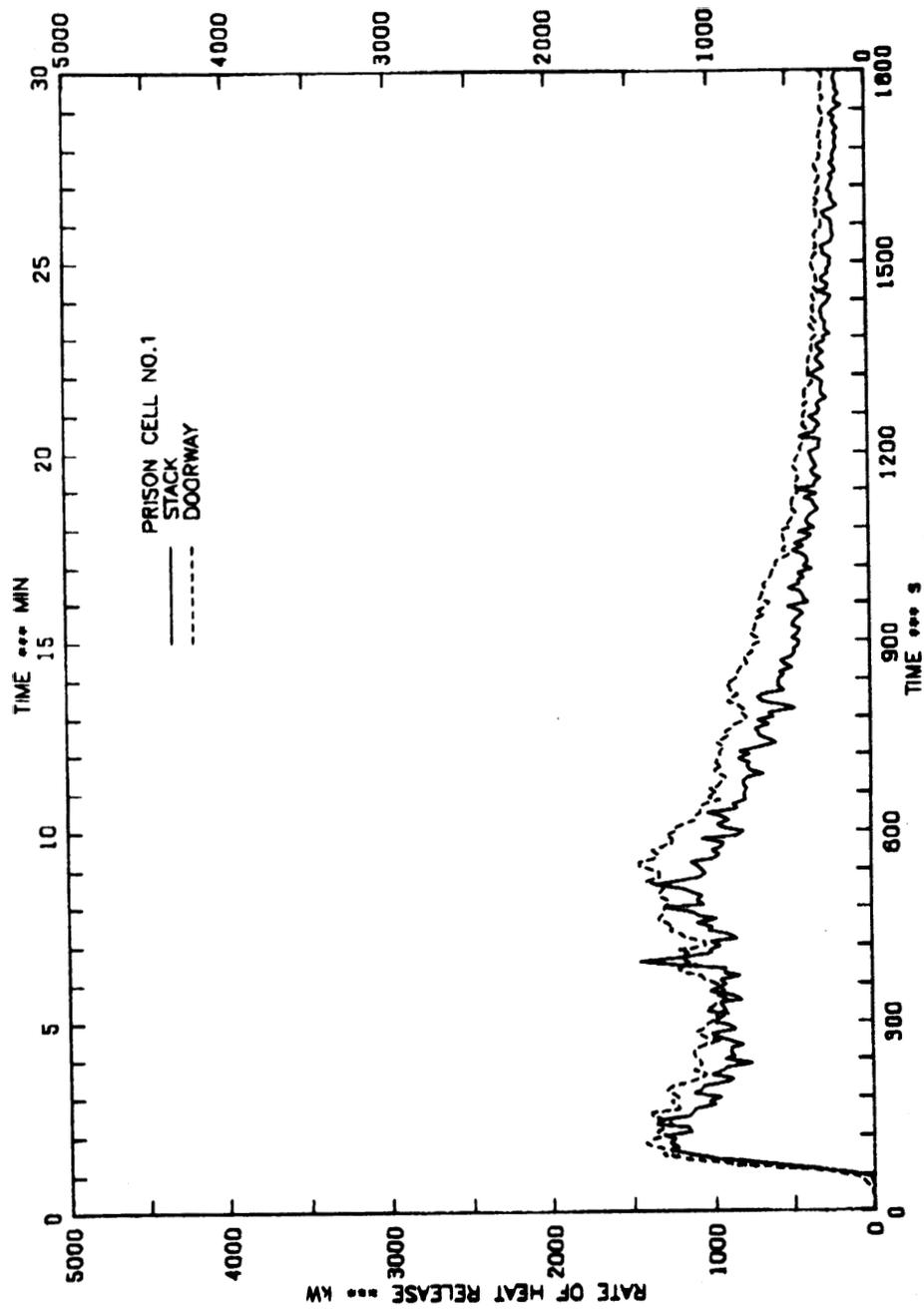
FIGURE 10 - HEAT RELEASE RATE HISTORY FOR CELL ROOM TEST 1
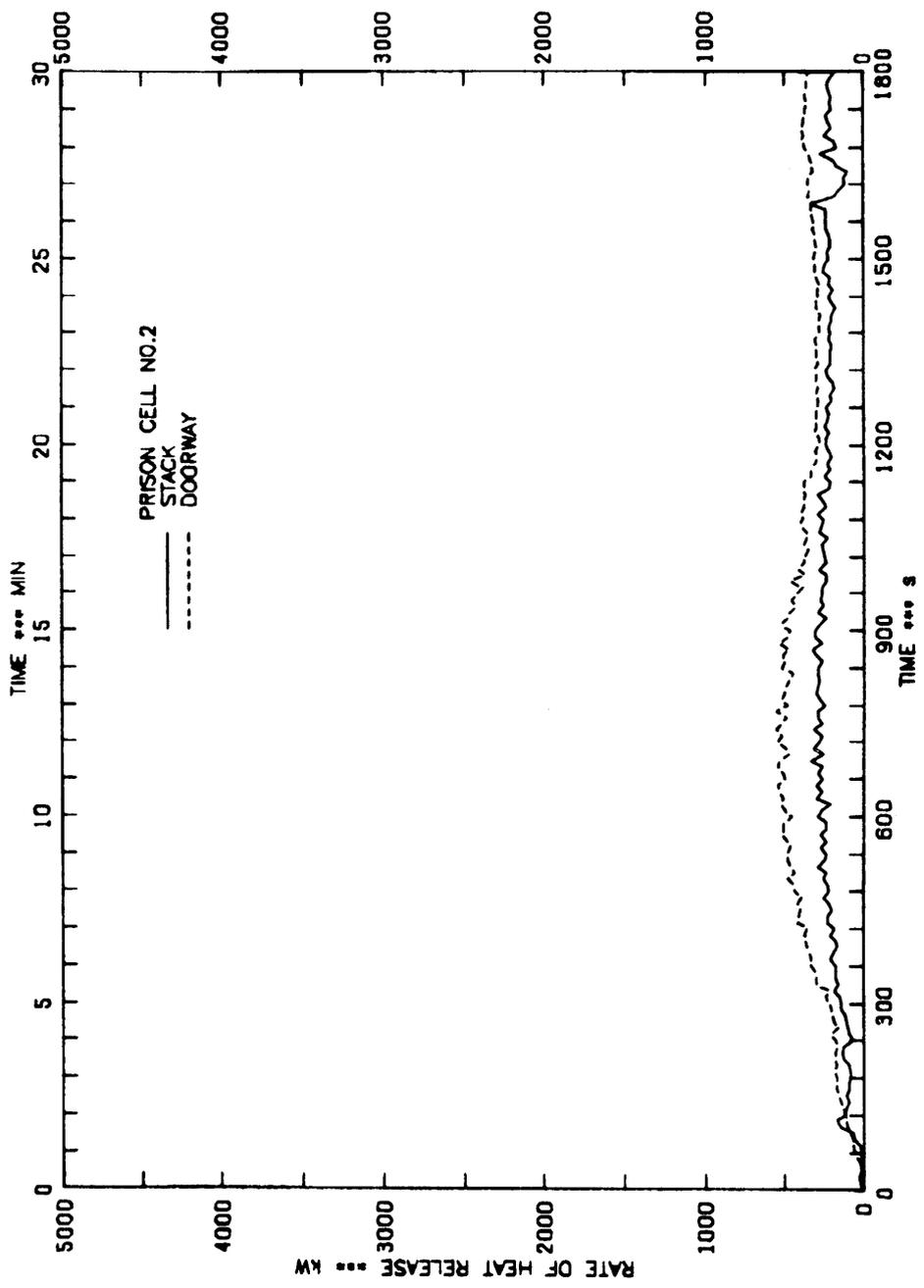
FIGURE 11 — HEAT RELEASE RATE HISTORY FOR CELL ROOM TEST 2

39
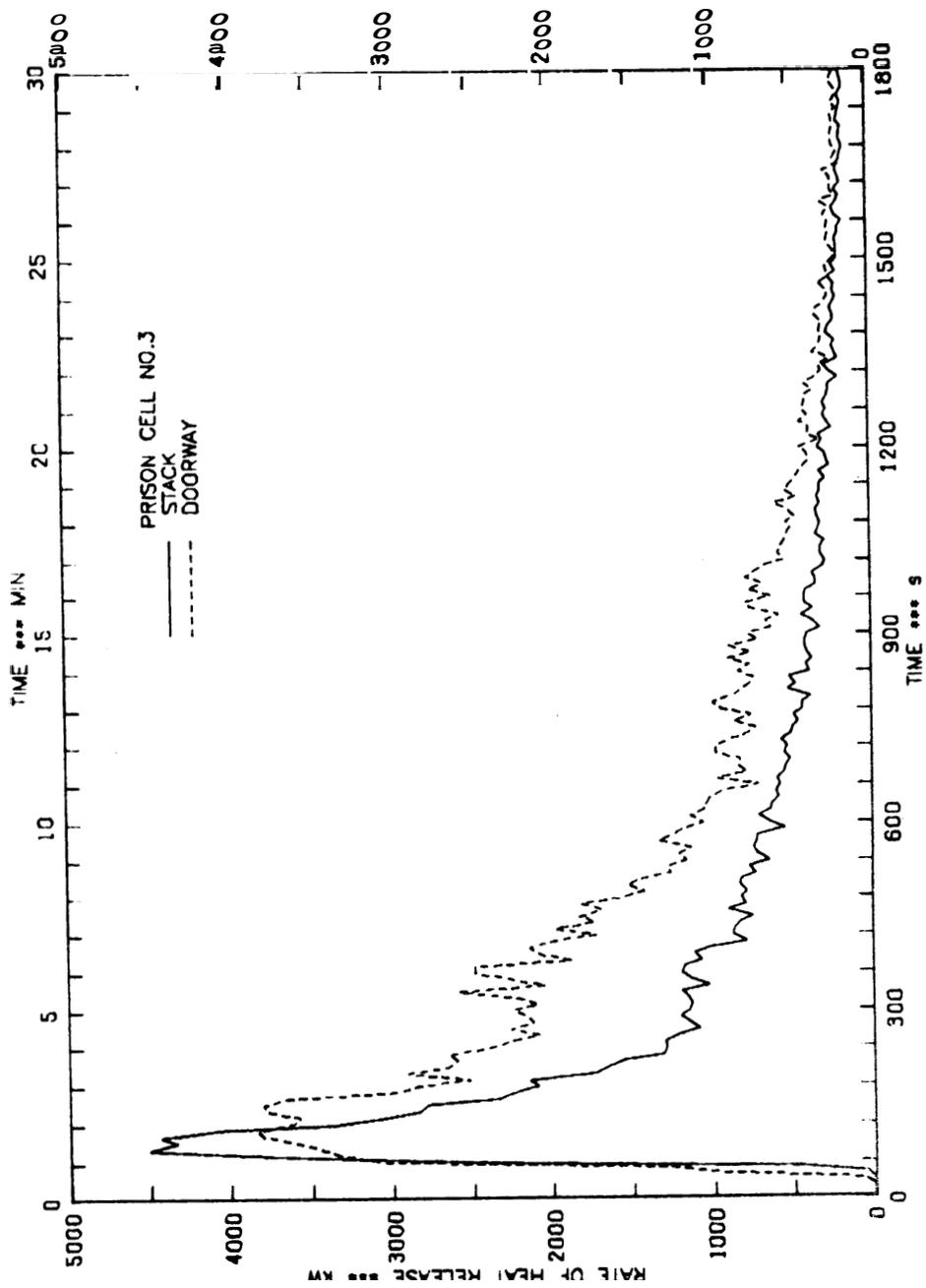
FIGURE 12 — HEAT RELEASE RATE HISTORY FOR CELL ROOM TEST 3
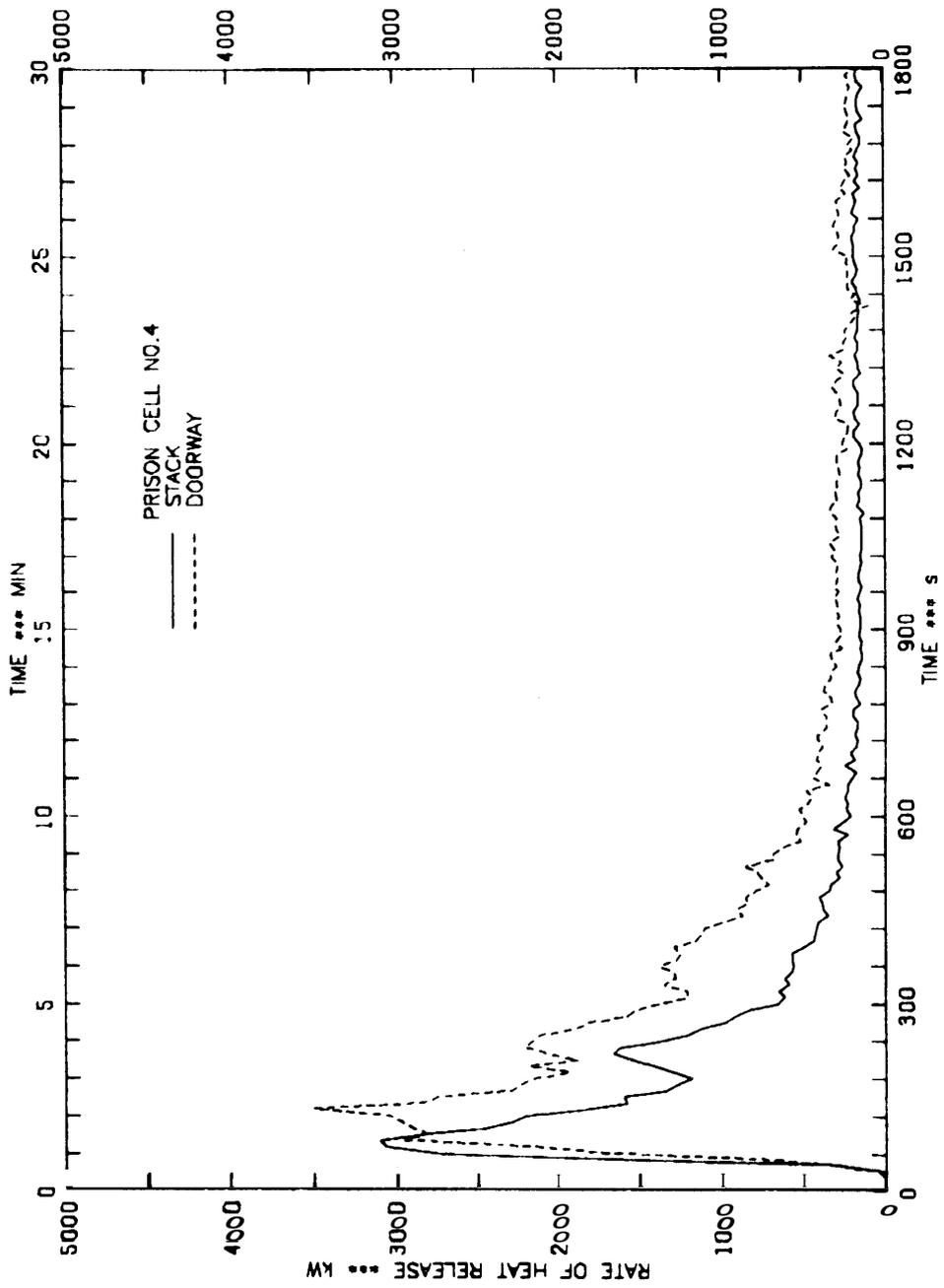
FIGURE 13 - HEAT RELEASE RATE HISTORY FOR CELL ROOM TEST 4

41
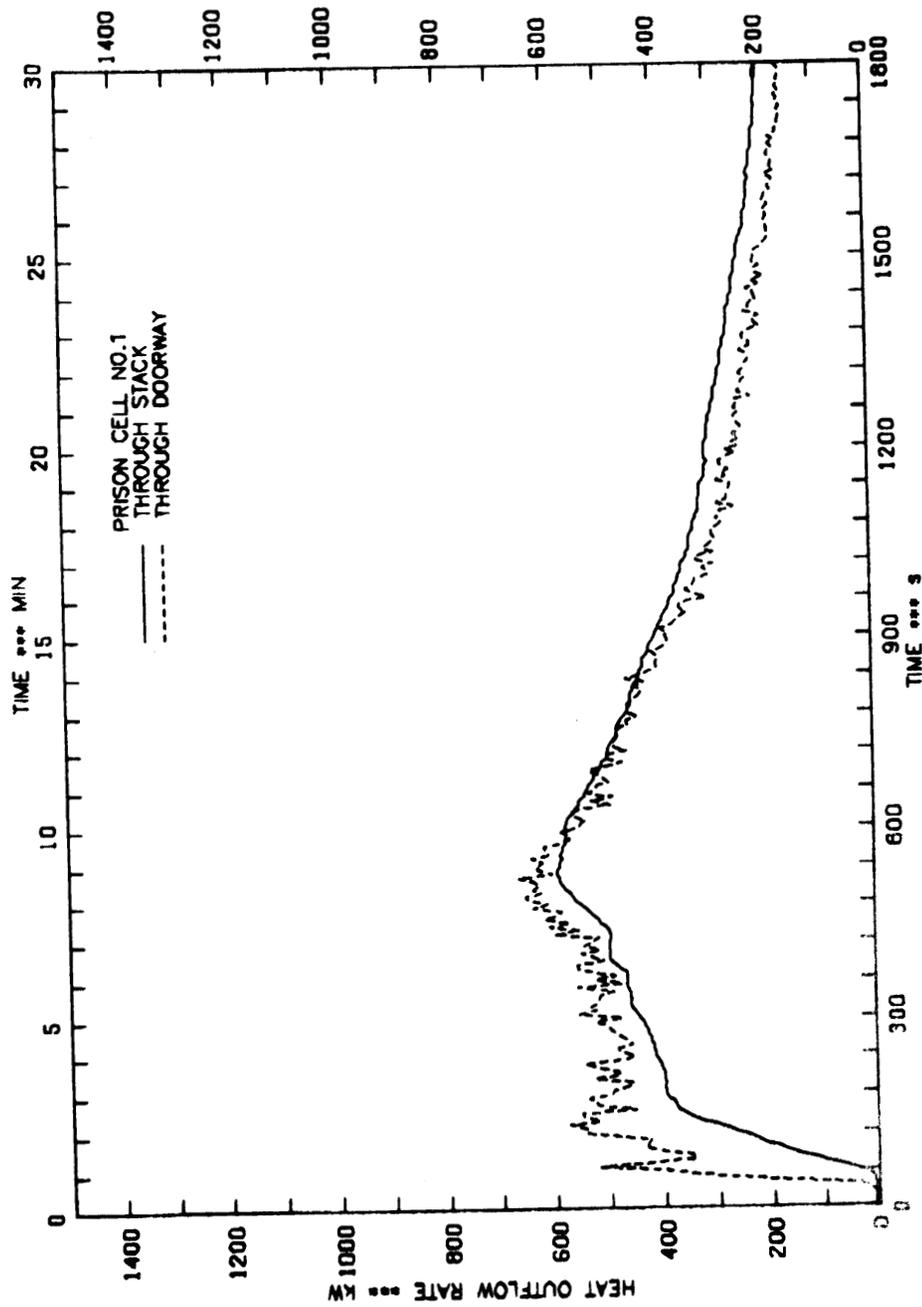
FIGURE 14 - HEAT OUTFLOW RATE FROM CELL ROOM TEST 1

PRISON CELL NO.1
THROUGH STACK
THROUGH DOORWAY

TIME ... MIN

TIME ... S

HEAT OUTFLOW RATE ... kW
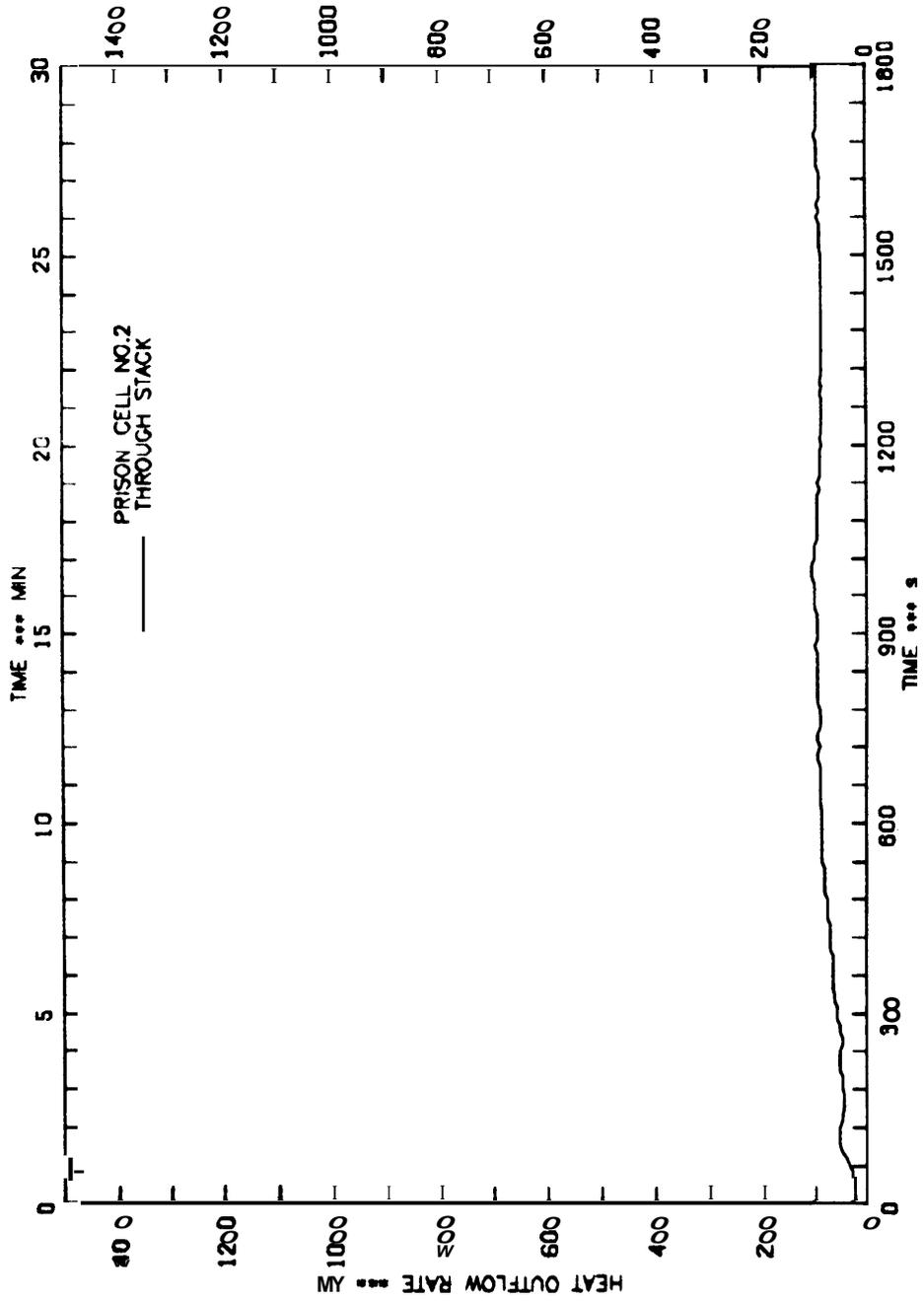
FIGURE 15 - HEAT OUTFLOW RATE FROM CELL ROOM TEST 2

PRISON CELL NO.2
THROUGH STACK

43
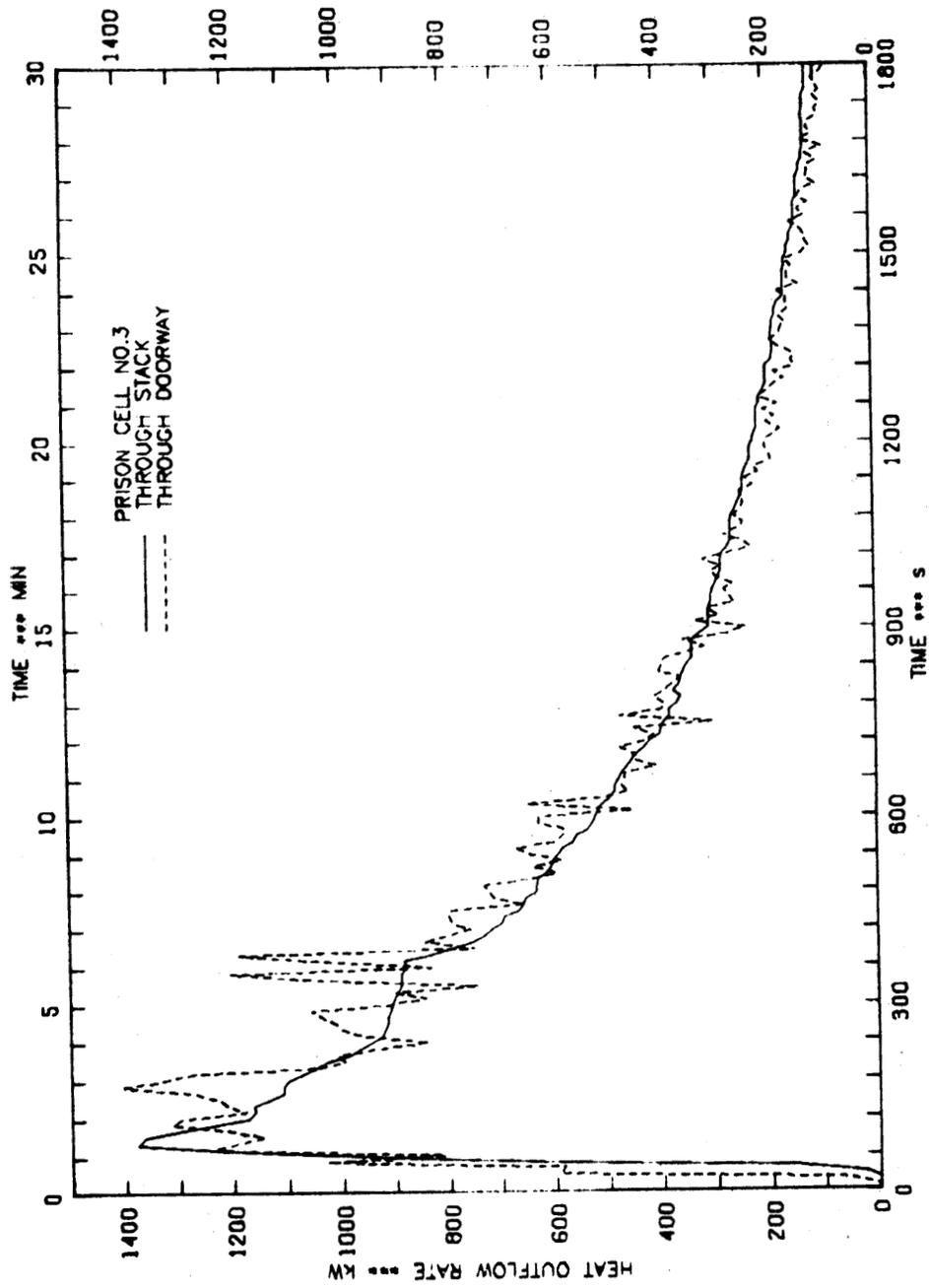
FIGURE 16 — HEAT OUTFLOW RATE FROM CELL ROOM TEST 3
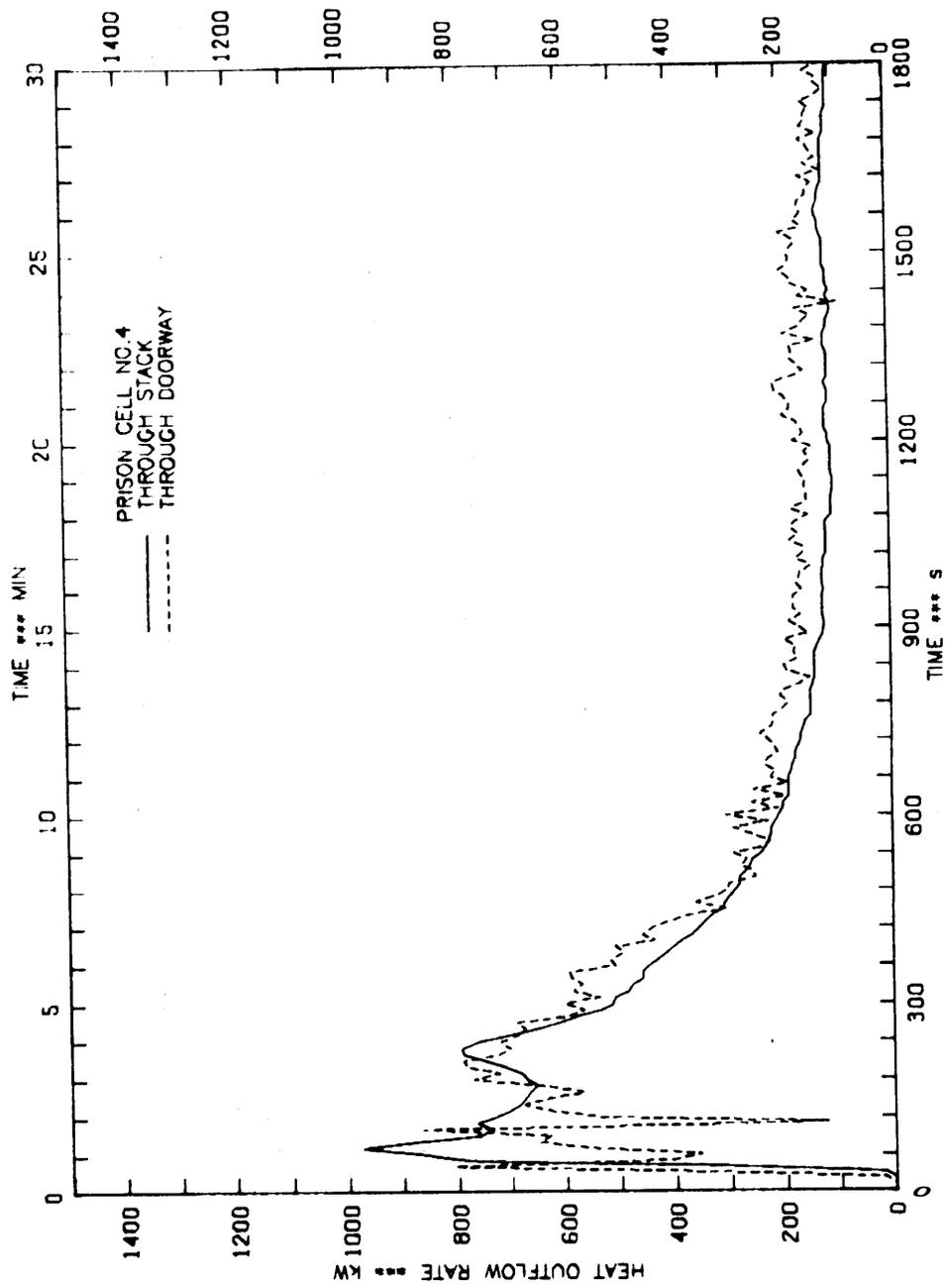
FIGURE 17 - HEAT OUTFLOW RATE FROM CELL ROOM TEST 4

45
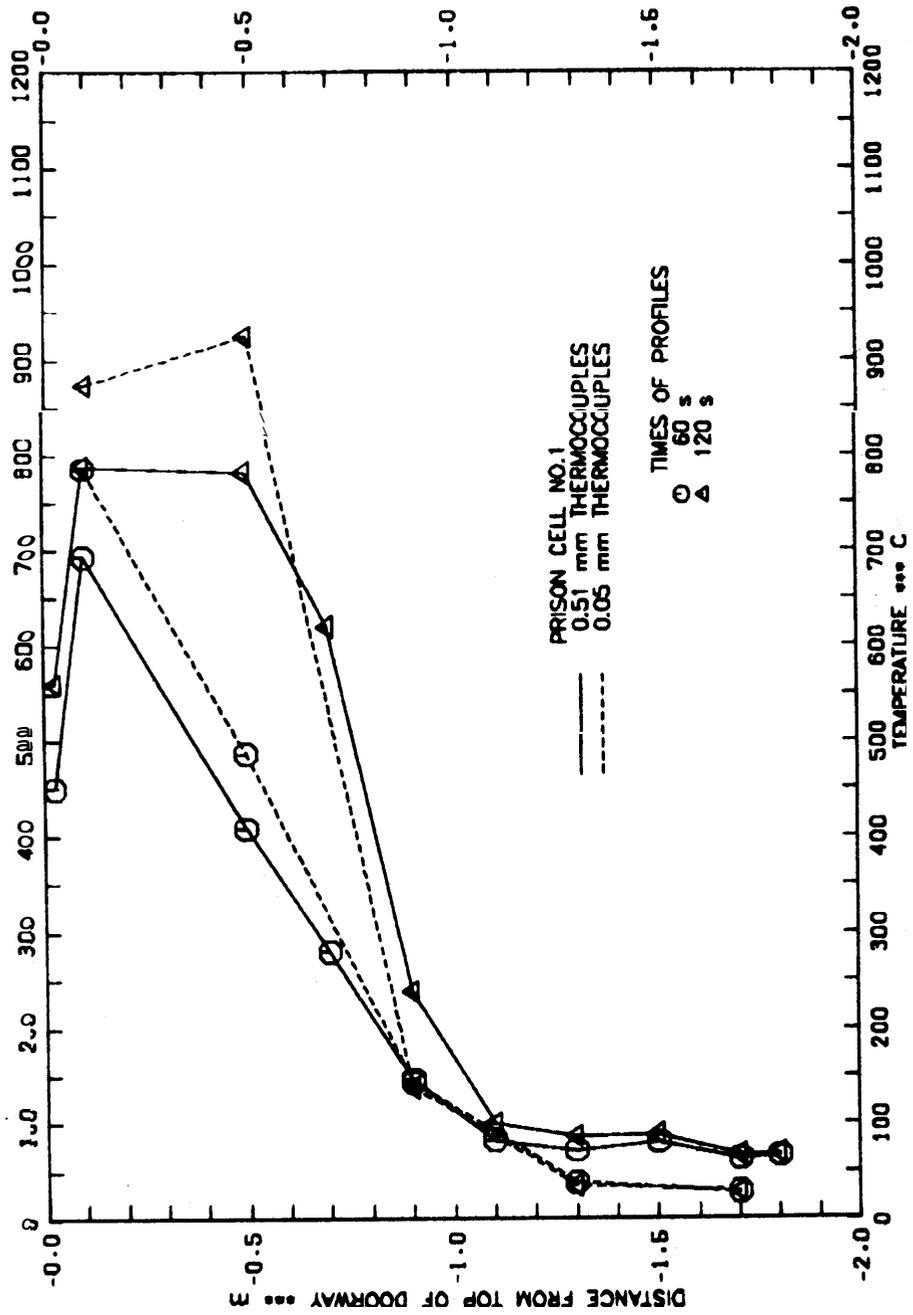
FIGURE 16A – DOORWAY AIR TEMPERATURE PROFILES FOR TEST 1
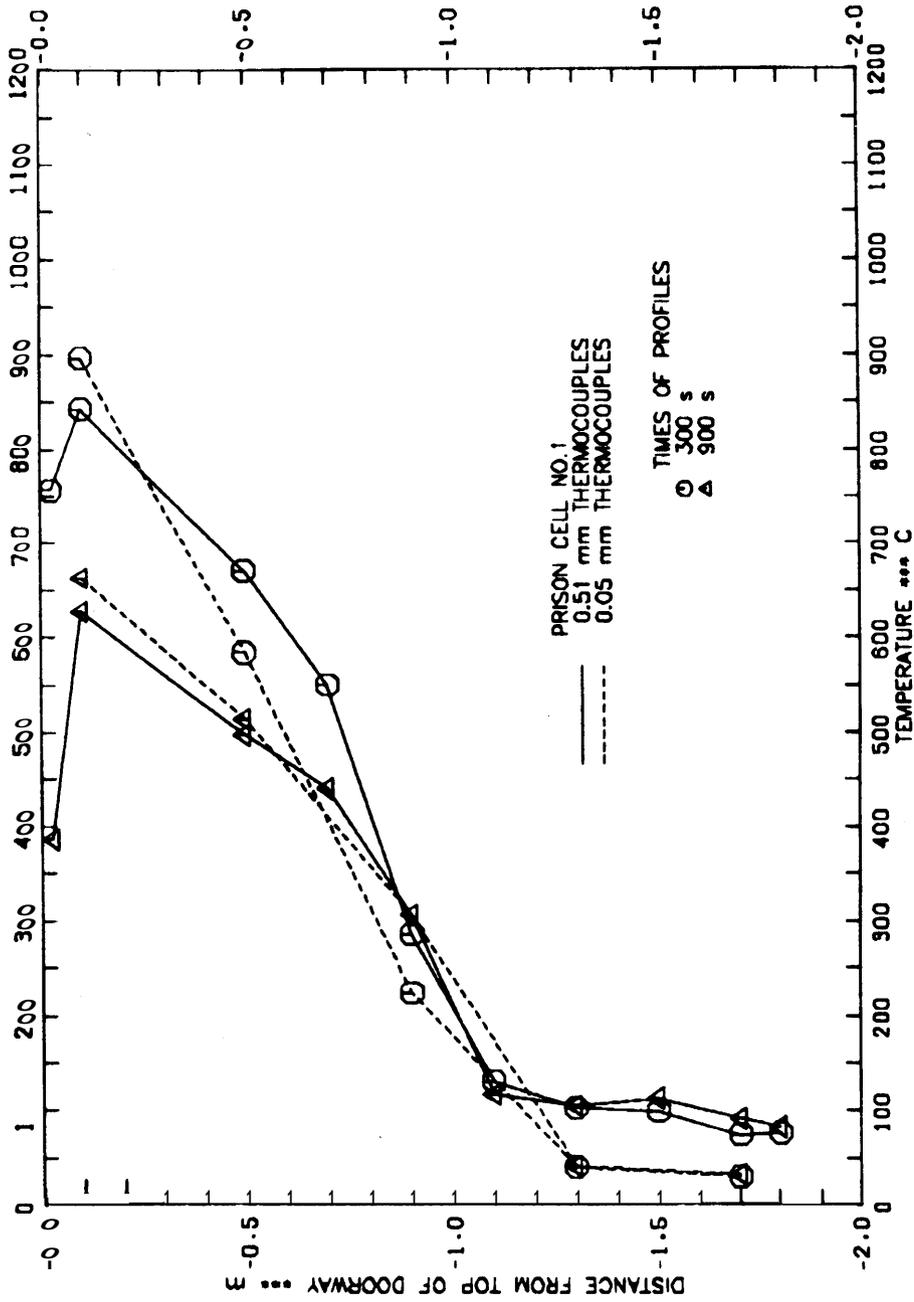
FIGURE 18.8 - DOORWAY AIR TEMPERATURE PROFILES FOR TEST 1

PRISON CELL NO.1
    0.51 mm THERMOCOUPLES
    0.05 mm THERMOCOUPLES

TIMES OF PROFILES
    ⊙ 300 s
    △ 900 s

TEMPERATURE ••• C

DISTANCE FROM TOP OF DOORWAY ••• m
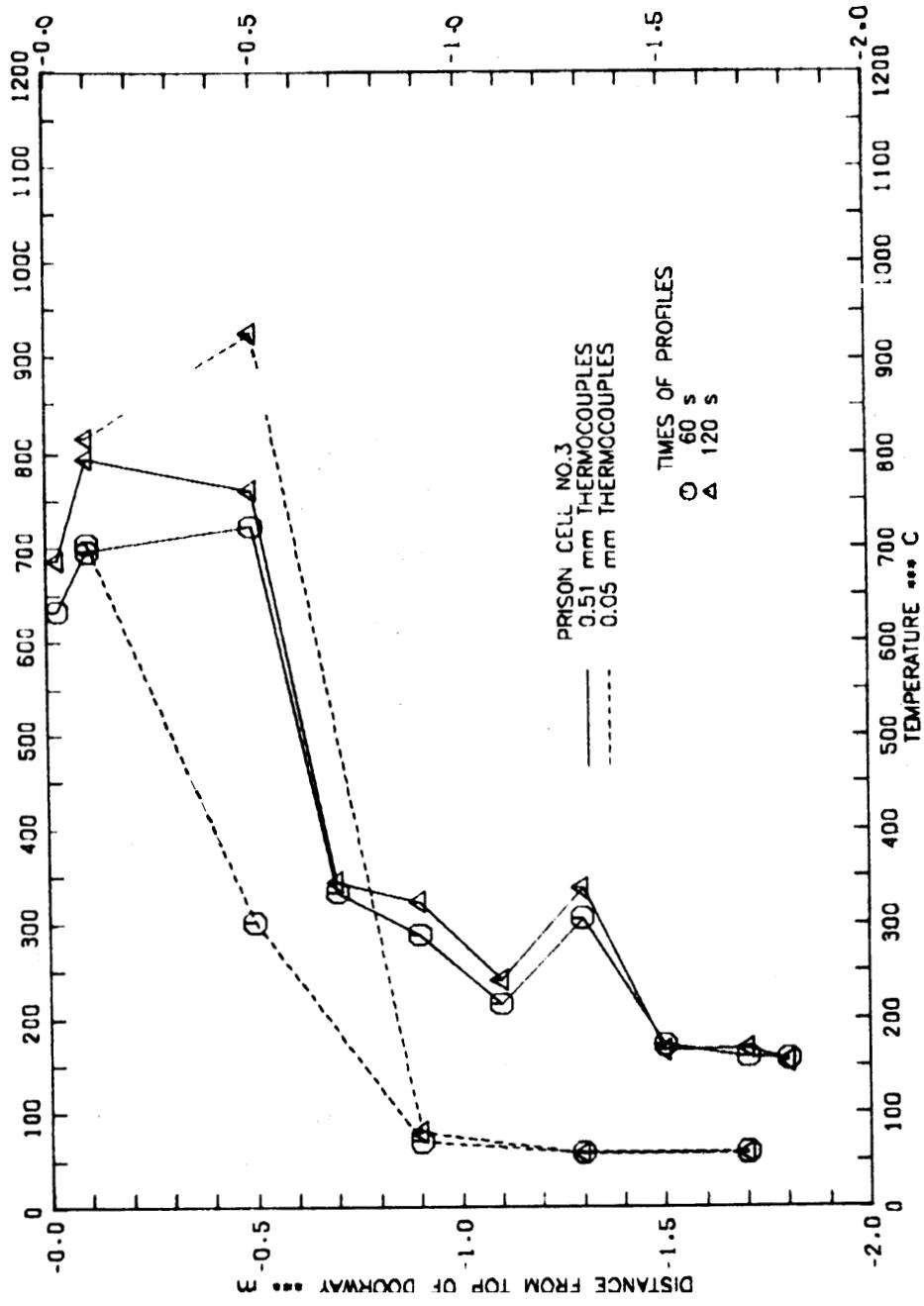
FIGURE 19.A — DOORWAY AIR TEMPERATURE PROFILES FOR TEST 3
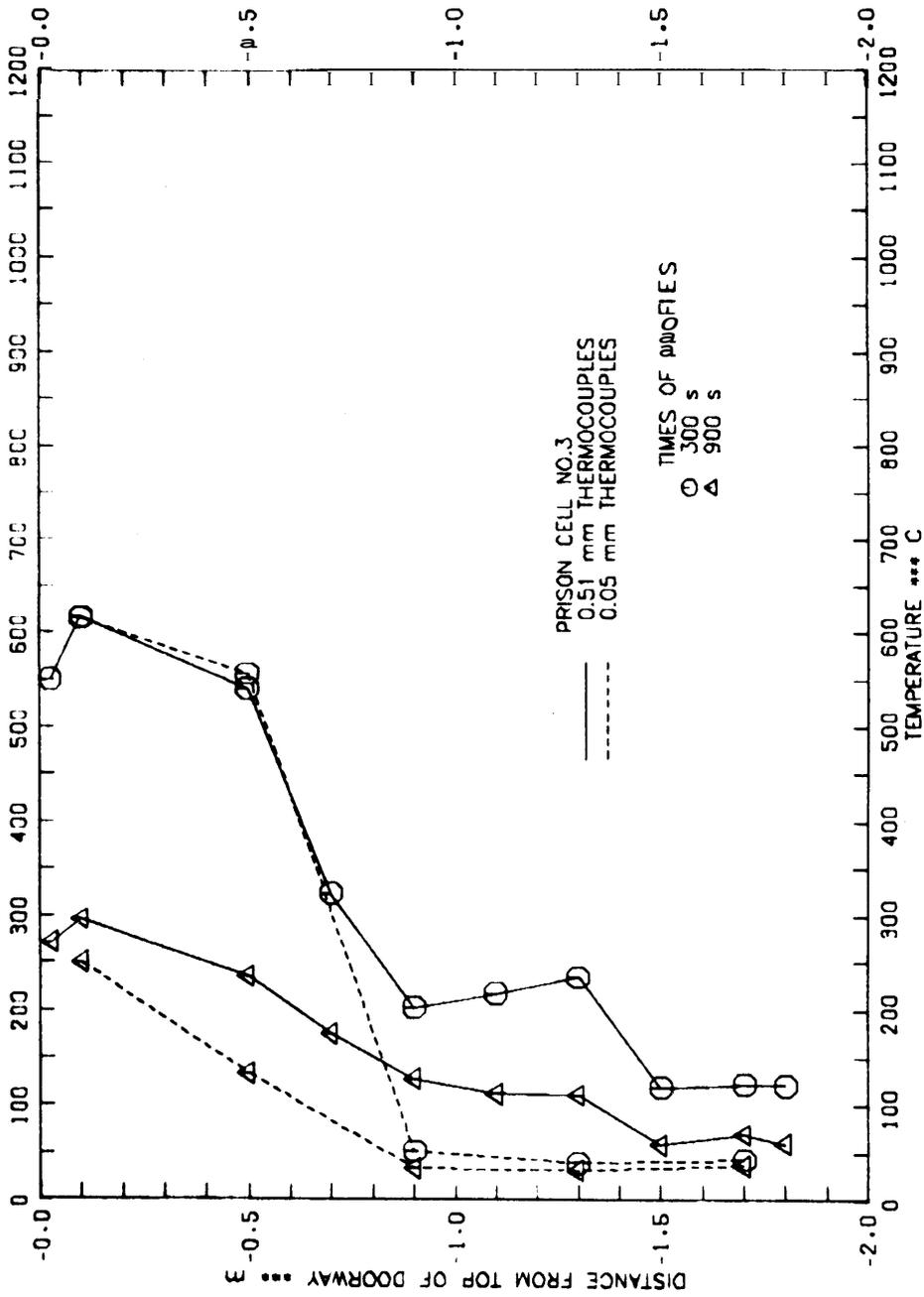
FIGURE 19.B — DOORWAY AIR TEMPERATURE PROFILES FOR TEST 3

PRISON CELL NO.3
0.51 mm THERMOCOUPLES
0.05 mm THERMOCOUPLES

TIMES OF PROFILES
⊙ 300 s
△ 900 s

TEMPERATURE ••• C

DISTANCE FROM TOP OF DOORWAY ••• m

49
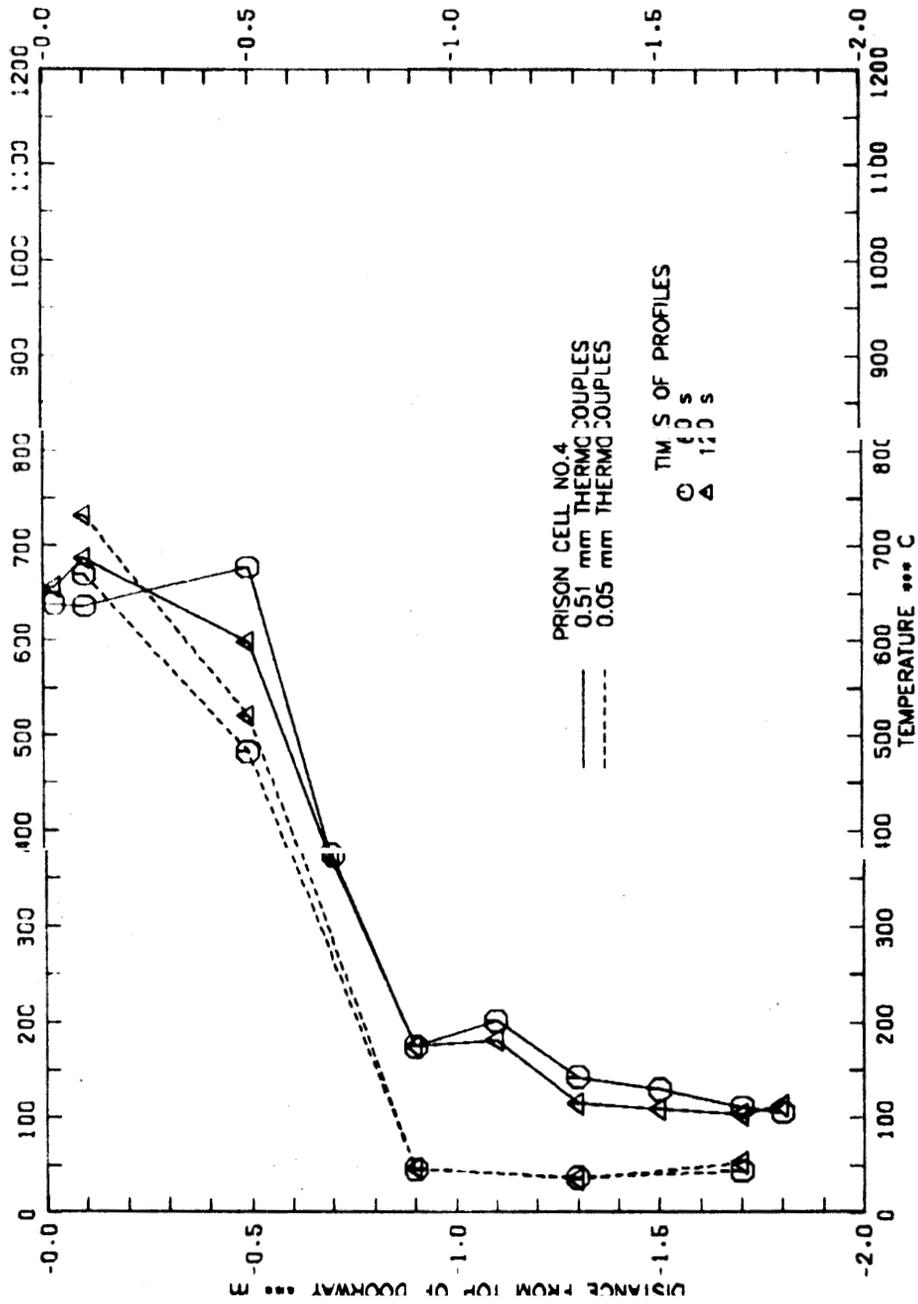
FIGURE 20A – DOORWAY AIR TEMPERATURE PROFILES FOR TEST 4

PRISON CELL NO.4
——— 0.51 mm THERMO COUPLES
- - - - 0.05 mm THERMO COUPLES

TIMES OF PROFILES
⊙ 60 s
△ 120 s

TEMPERATURE ••• C

DISTANCE FROM TOP OF DOORWAY ••• M
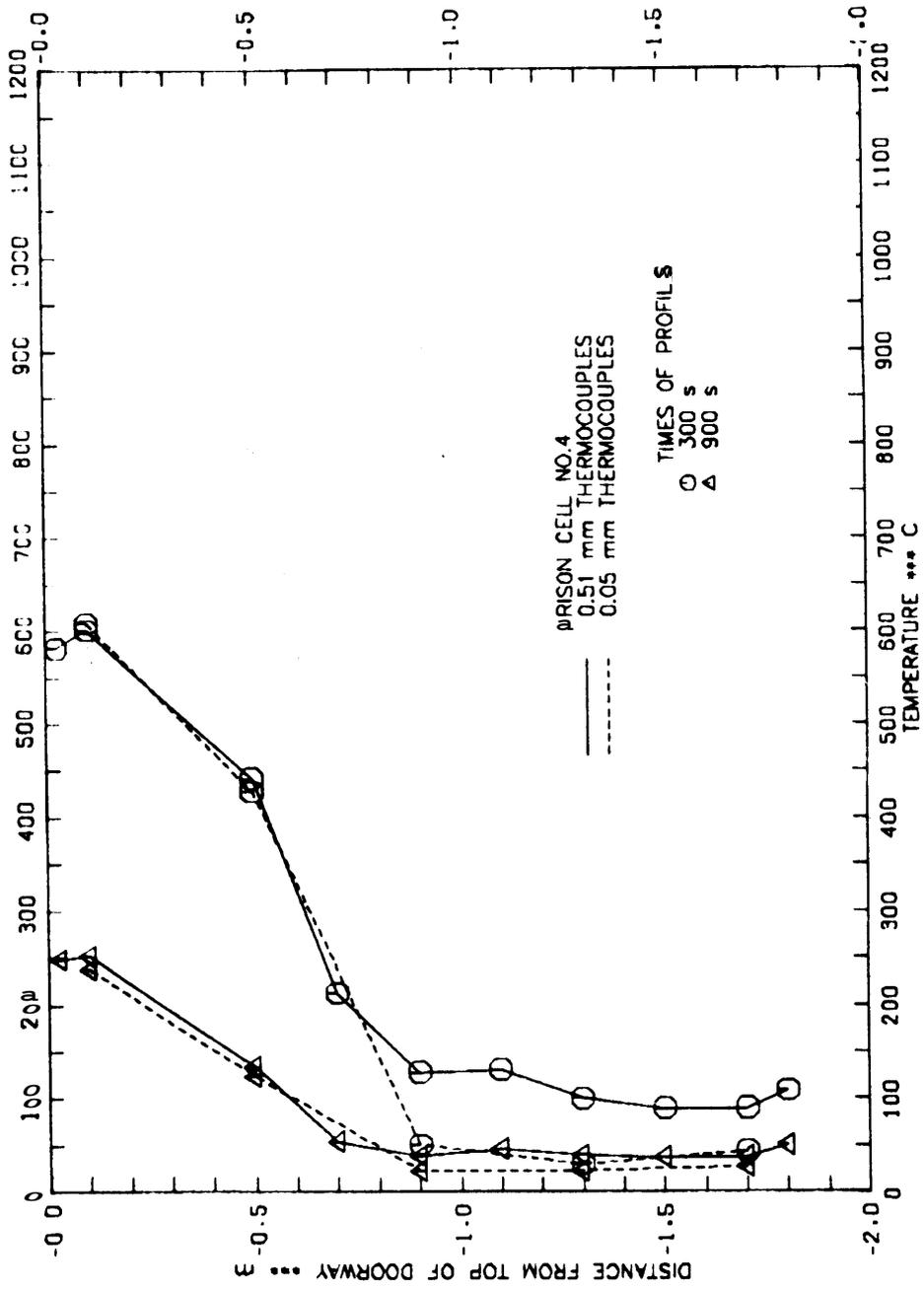
FIGURE 20.B - DOORWAY AIR TEMPERATURE PROFILES FOR TEST 4
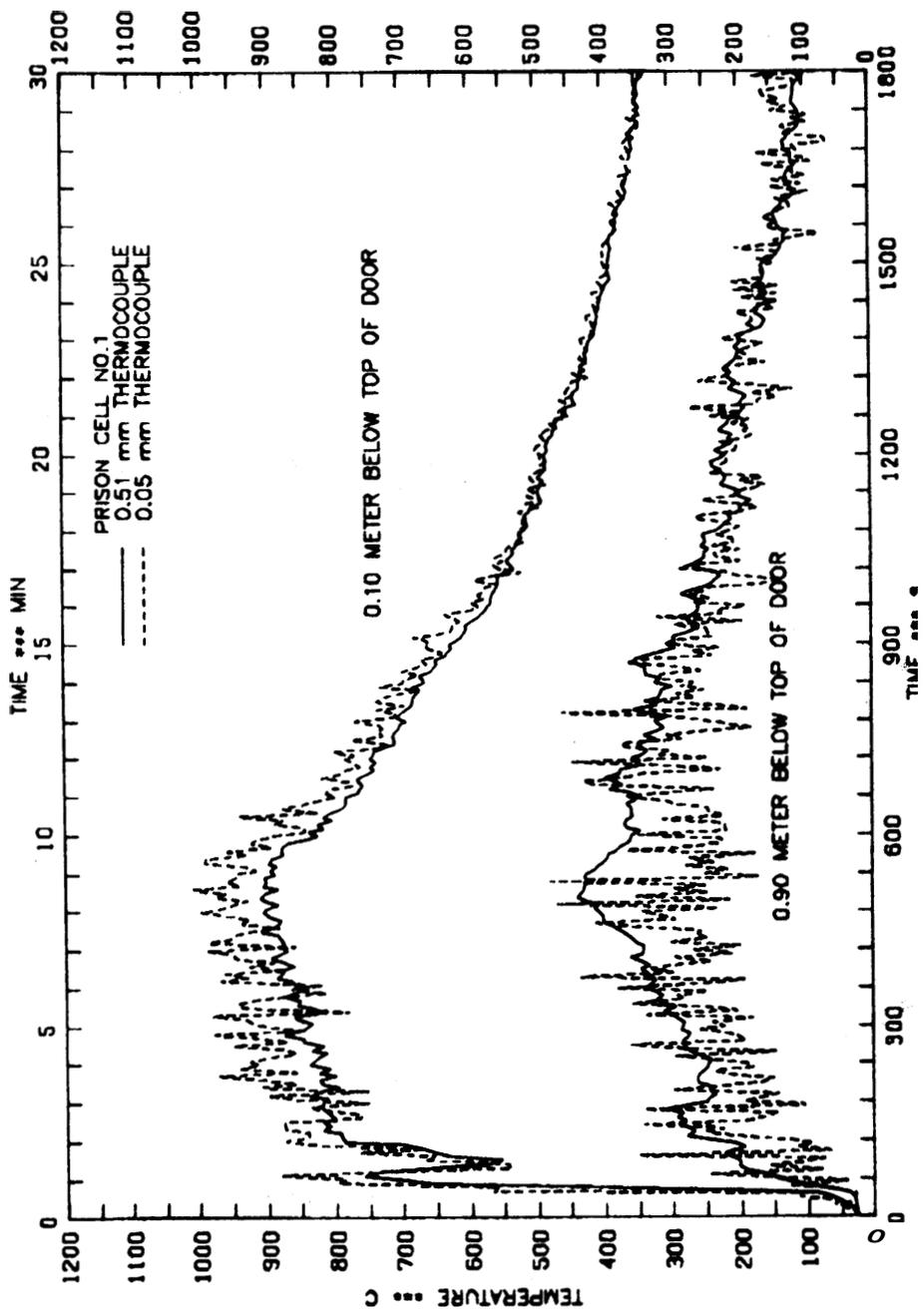
FIGURE 21.A — DOORWAY AIR TEMPERATURE HISTORIES FOR TEST 1
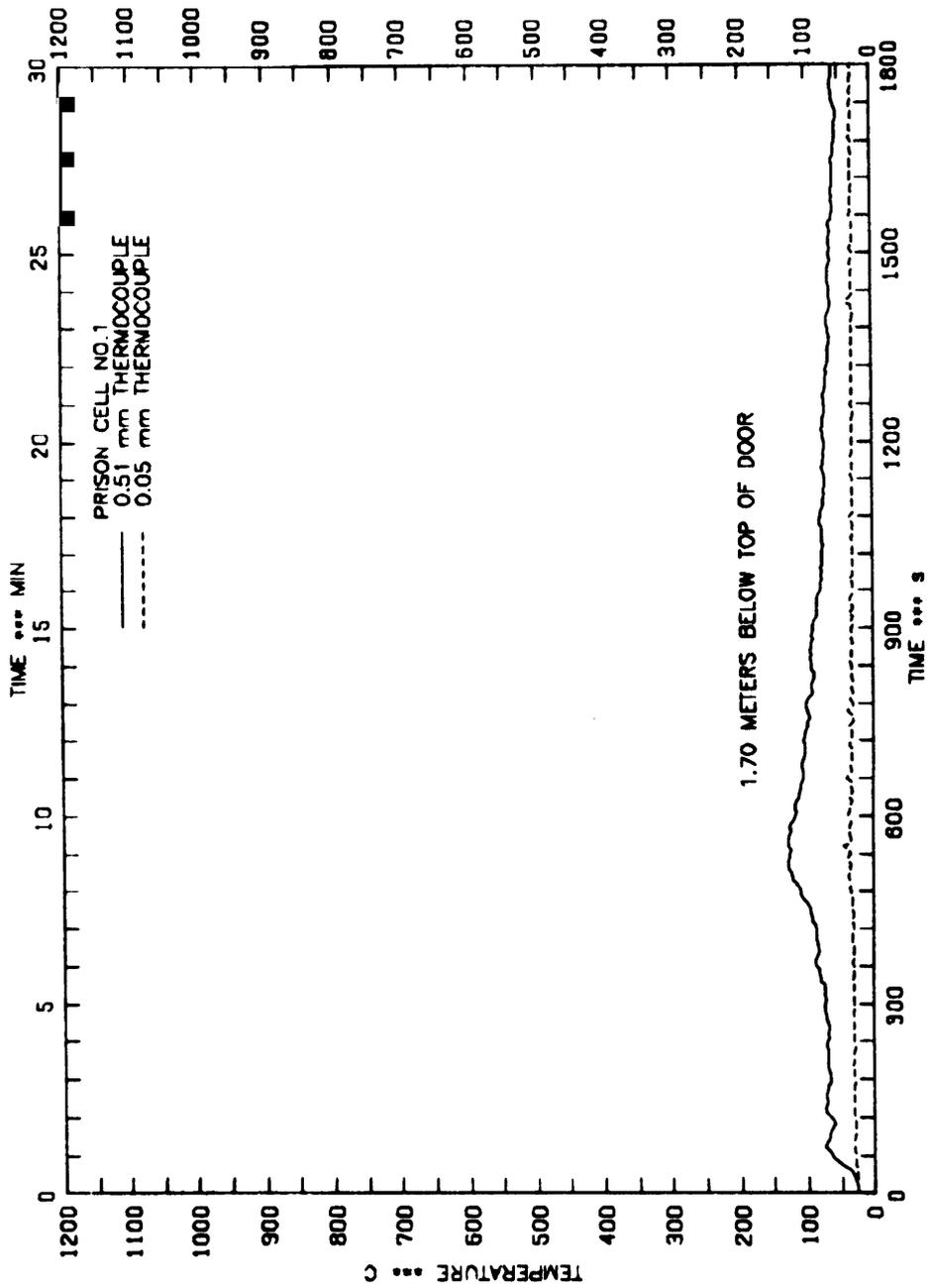
FIGURE 21.B - DOORWAY AIR TEMPERATURE HISTORIES FOR TEST 1

53
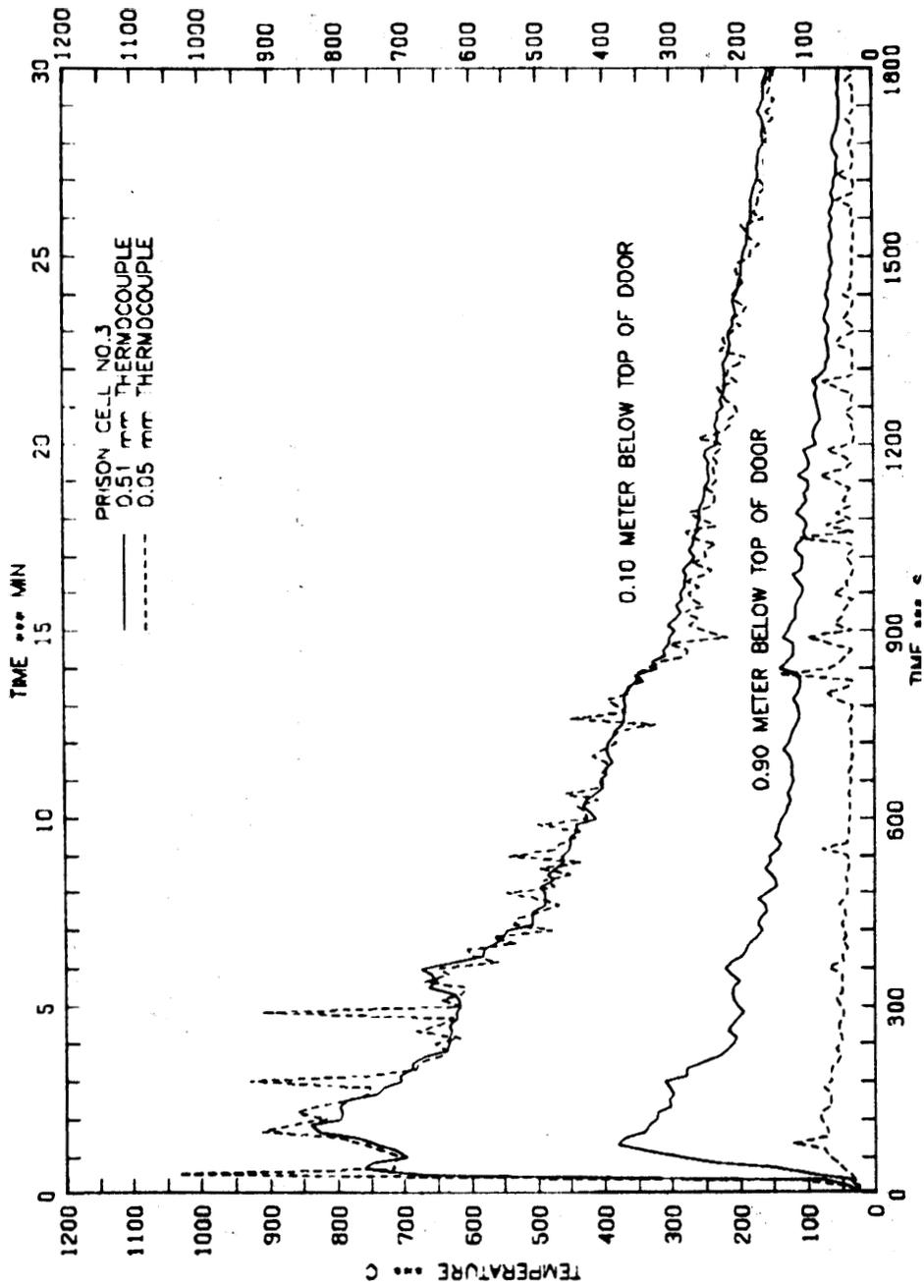
FIGURE 22.A - DOORWAY AIR TEMPERATURE HISTORIES FOR TEST 3

54
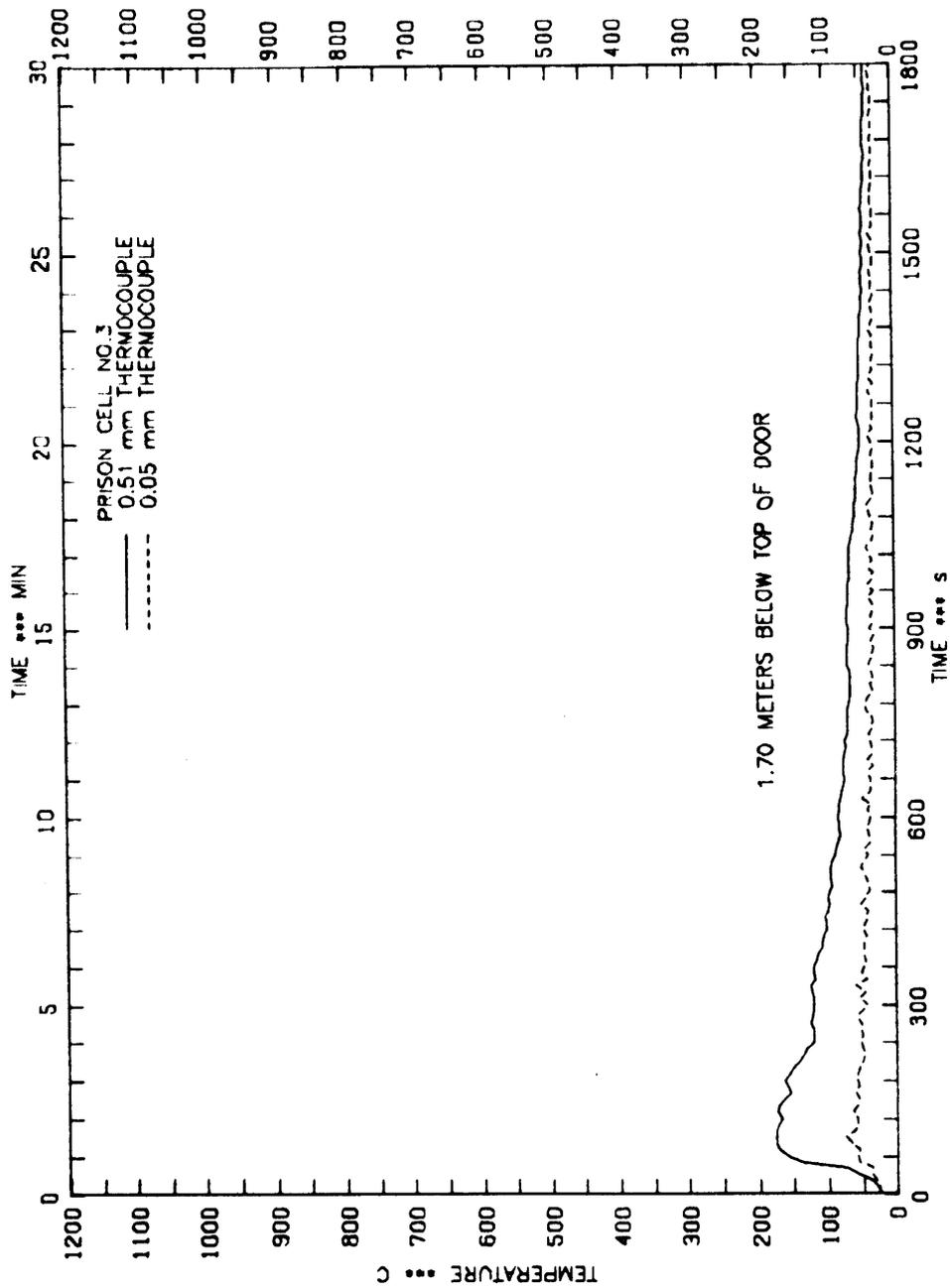
FIGURE 22.B – DOORWAY AIR TEMPERATURE HISTORIES FOR TEST 3
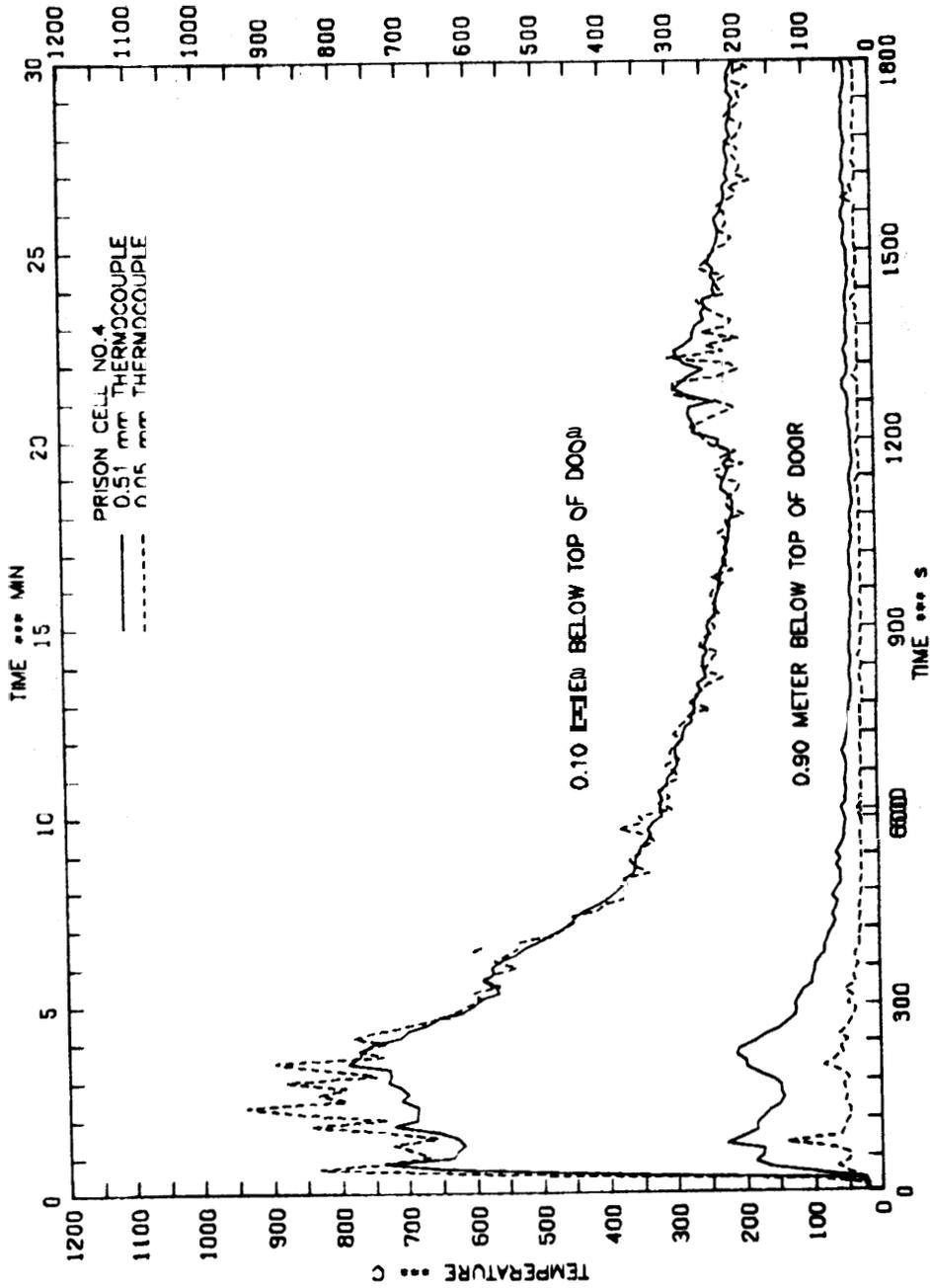
PRISON CELL NO.3
0.51 mm THERMOCOUPLE
0.05 mm THERMOCOUPLE

1.70 METERS BELOW TOP OF DOOR

TIME ••• MIN

TIME ••• s

TEMPERATURE ••• C

FIGURE 23.A — DOORWAY AIR TEMPERATURE HISTORIES FOR TEST 4
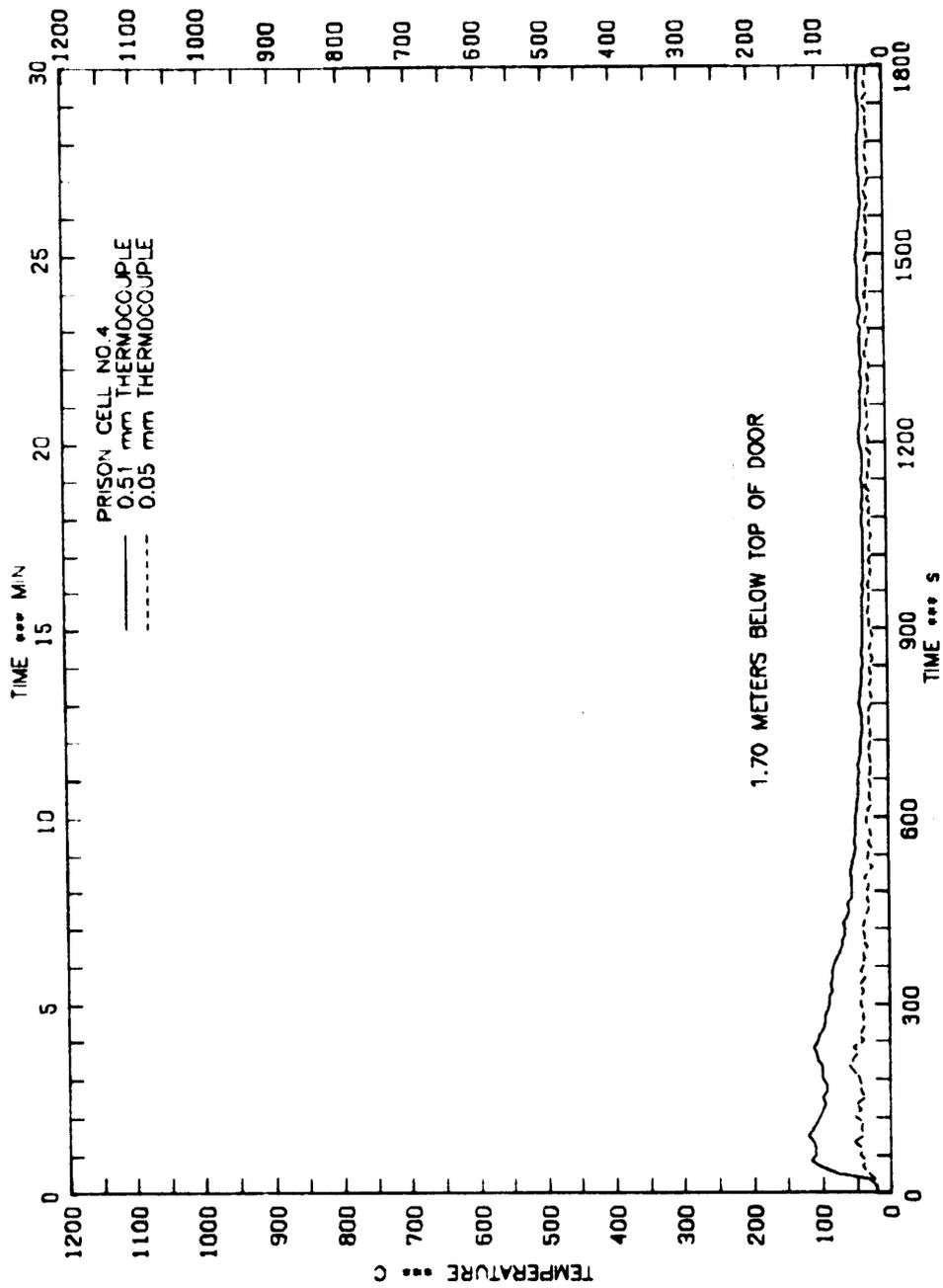
FIGURE 24 – DOORWAY AIR TEMPERATURE HISTORIES FOR TEST 4
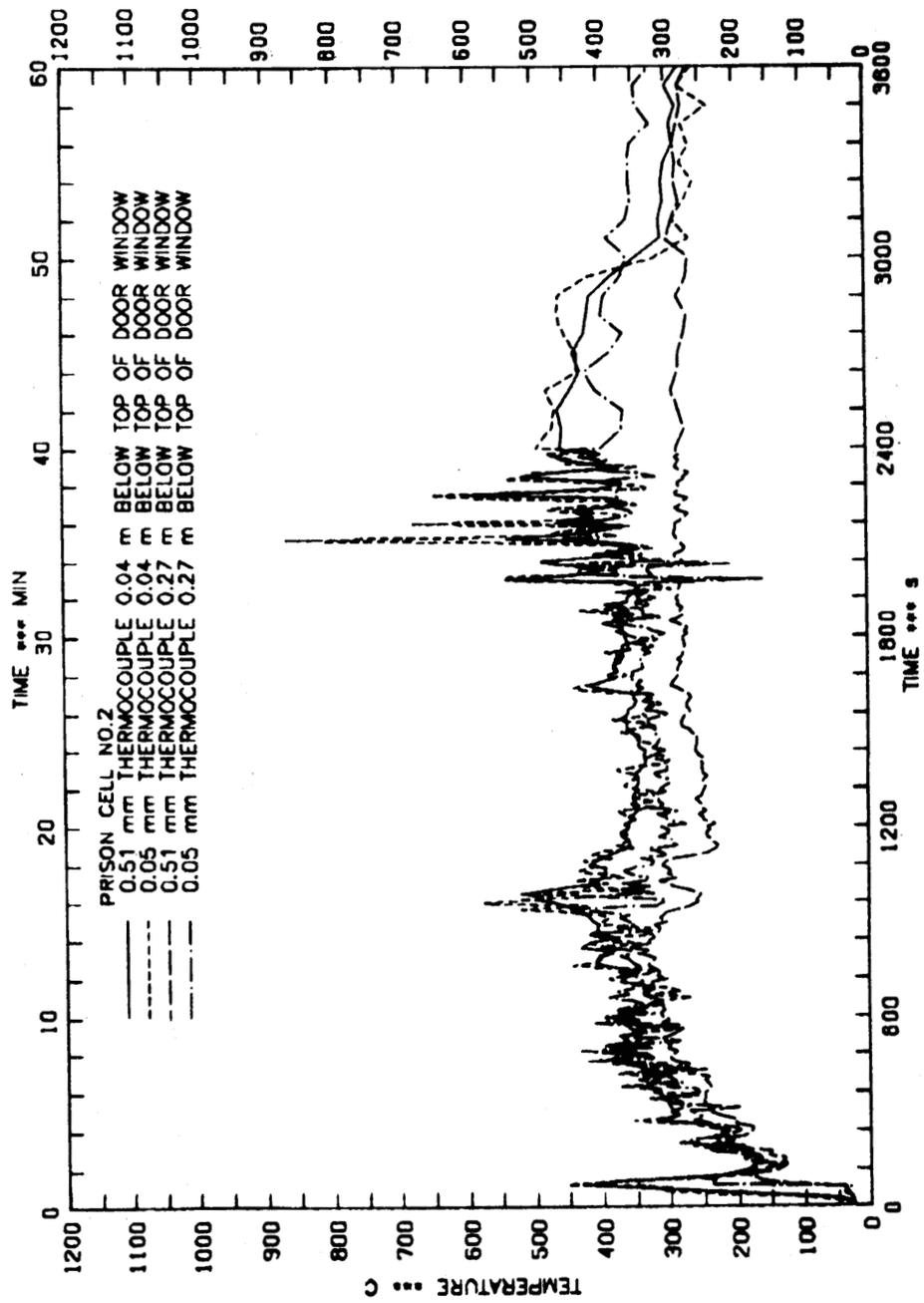
FIGURE 24 — DOORWAY AIR TEMPERATURE HISTORIES FOR TEST 2.

58
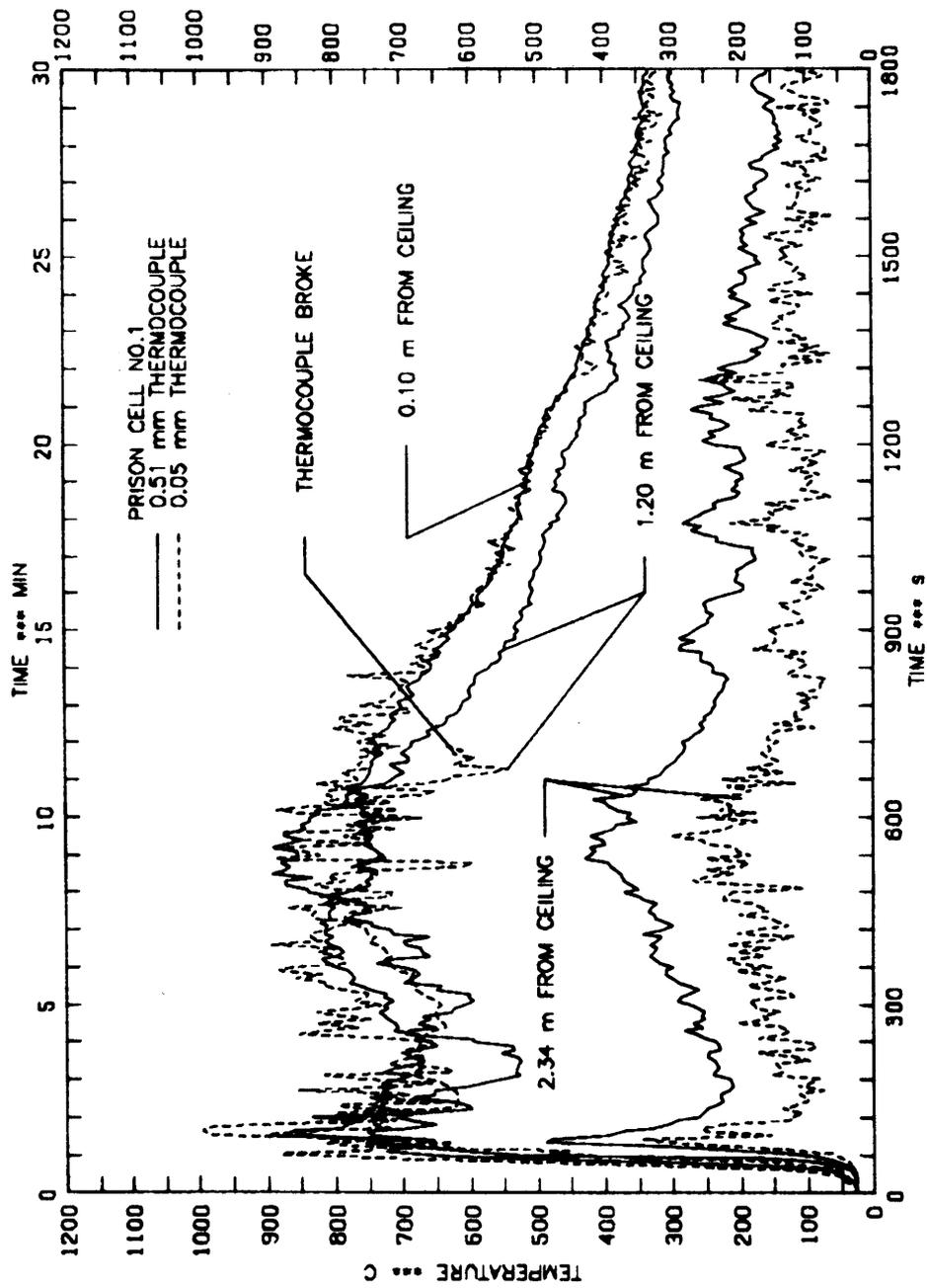
FIGURE 25 — INTERIOR AIR TEMPERATURE HISTORIES FOR TEST 1

PRISON CELL NO.1
0.51 mm THERMOCOUPLE
0.05 mm THERMOCOUPLE

THERMOCOUPLE BROKE

0.10 m FROM CEILING

1.20 m FROM CEILING

2.34 m FROM CEILING

TIME ••• MIN

TIME ••• s

TEMPERATURE ••• C

59
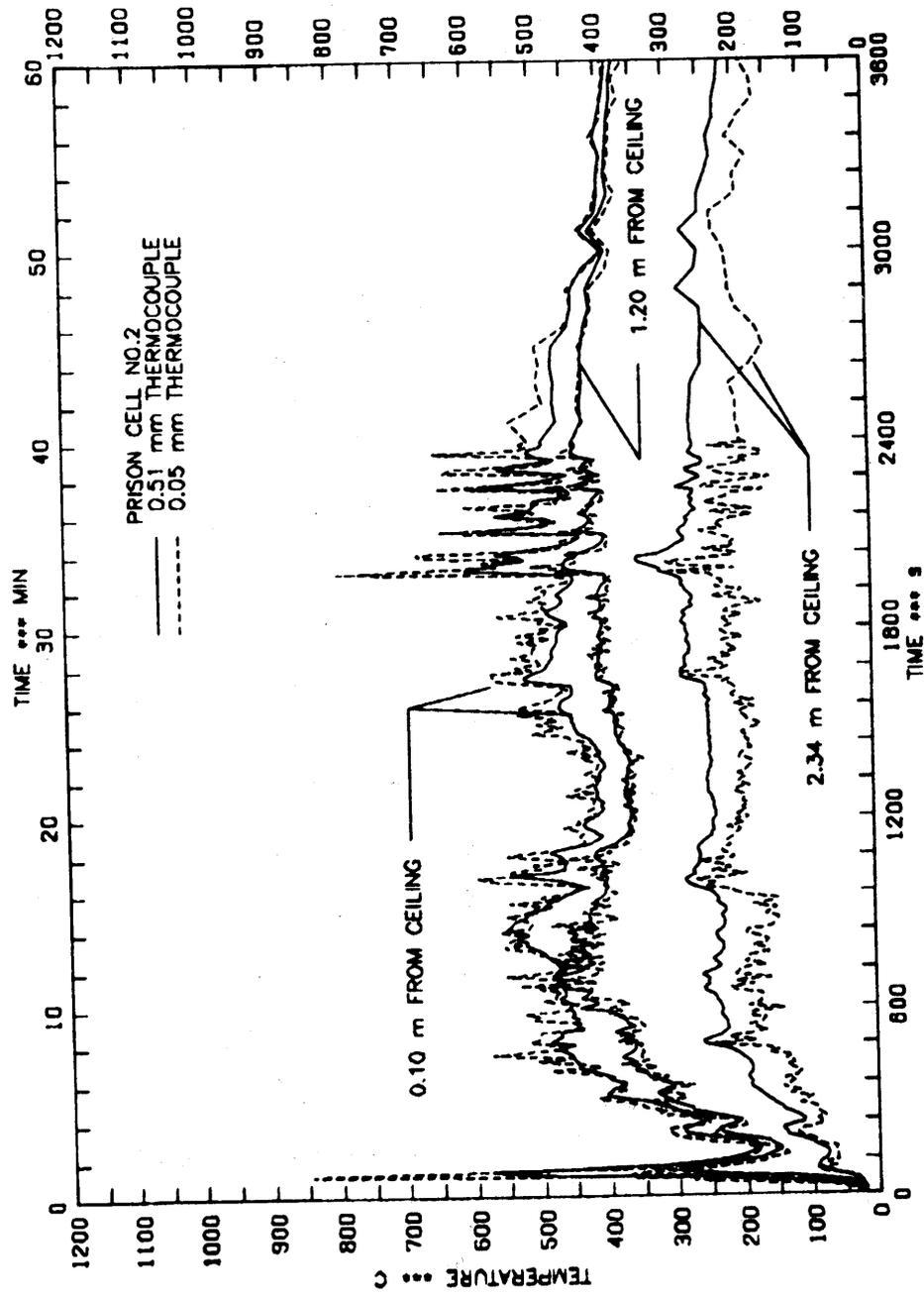
FIGURE 26 – INTERIOR AND TEMPERATURE HISTORIES FOR TEST Z
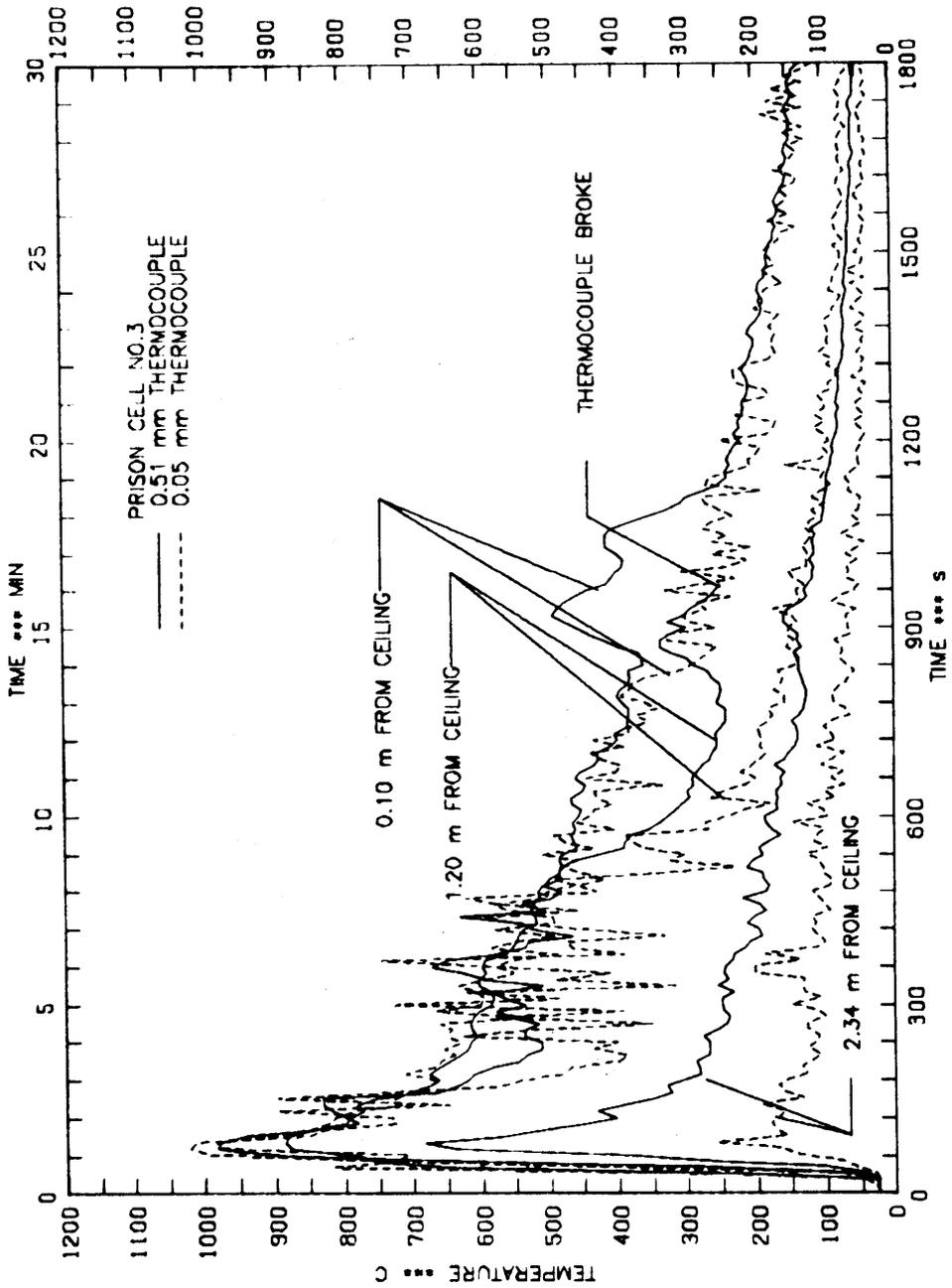
FIGURE 27 - INTERIOR AIR TEMPERATURE HISTORIES FOR TEST 3

61
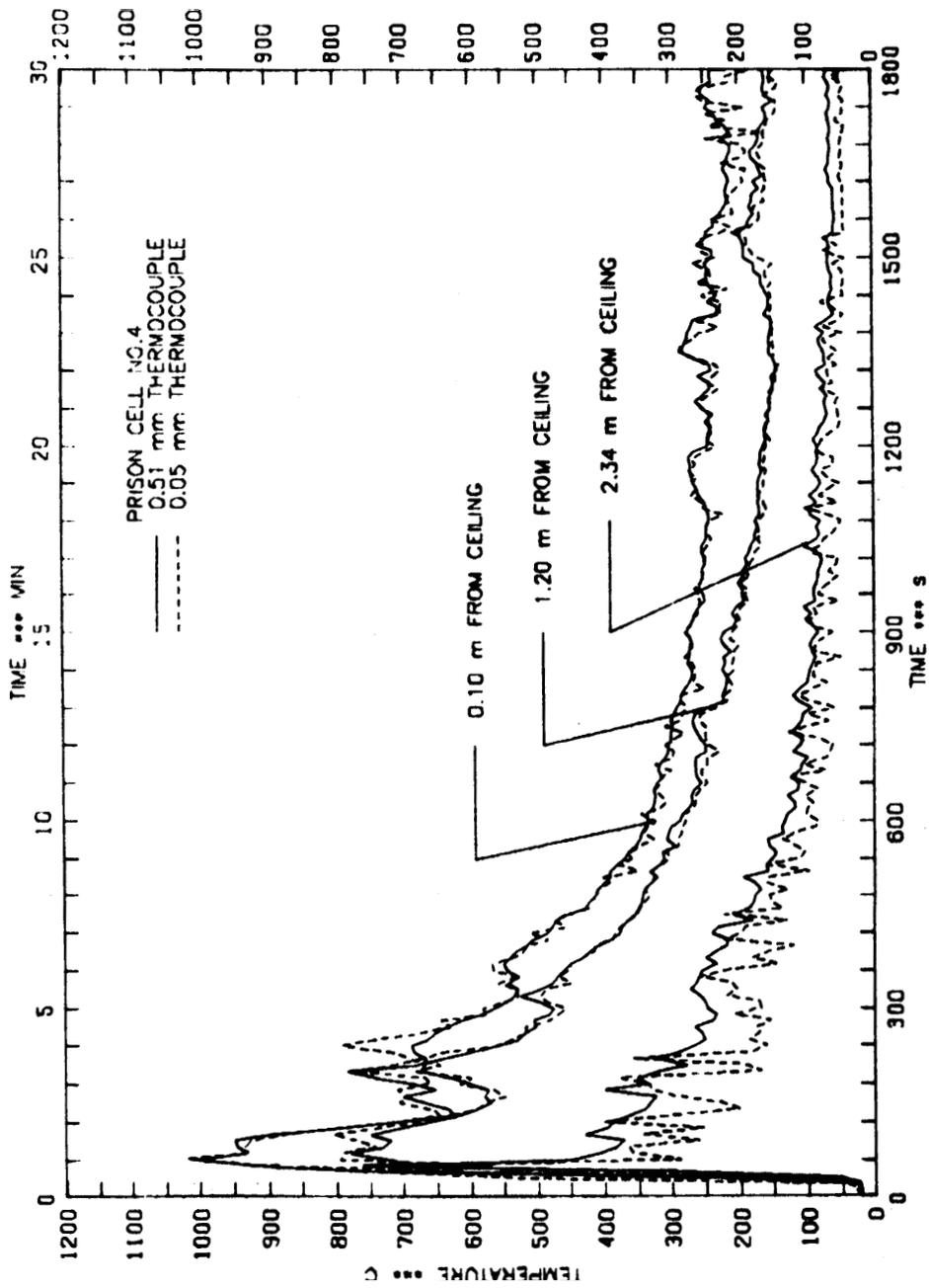
FIGURE 28 - INTERIOR AIR TEMPERATURE HISTORIES FOR TEST 4
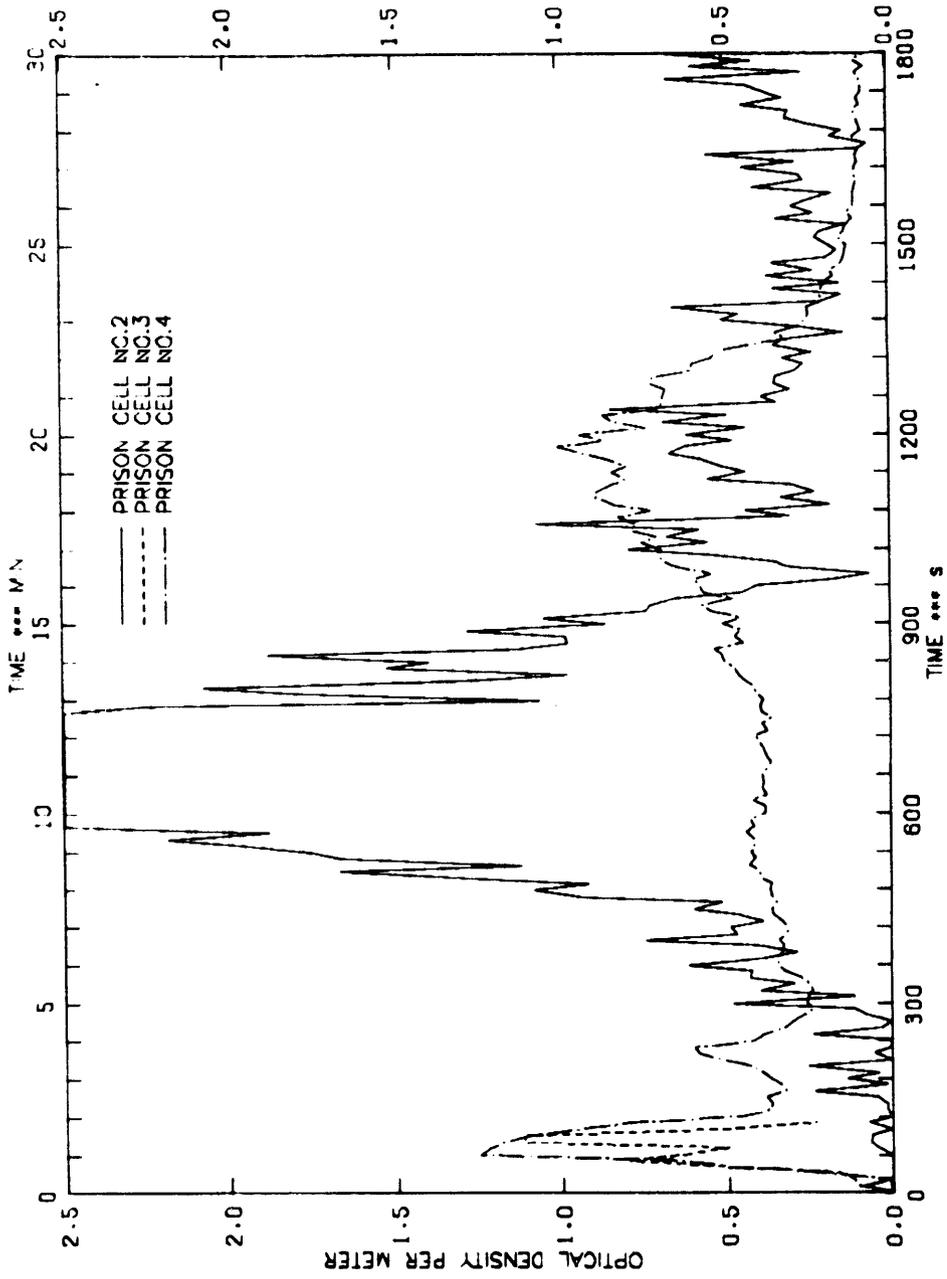
FIGURE 29 — SMOKE GENERATION HISTORIES FOR TESTS 2, 3 AND 4

63
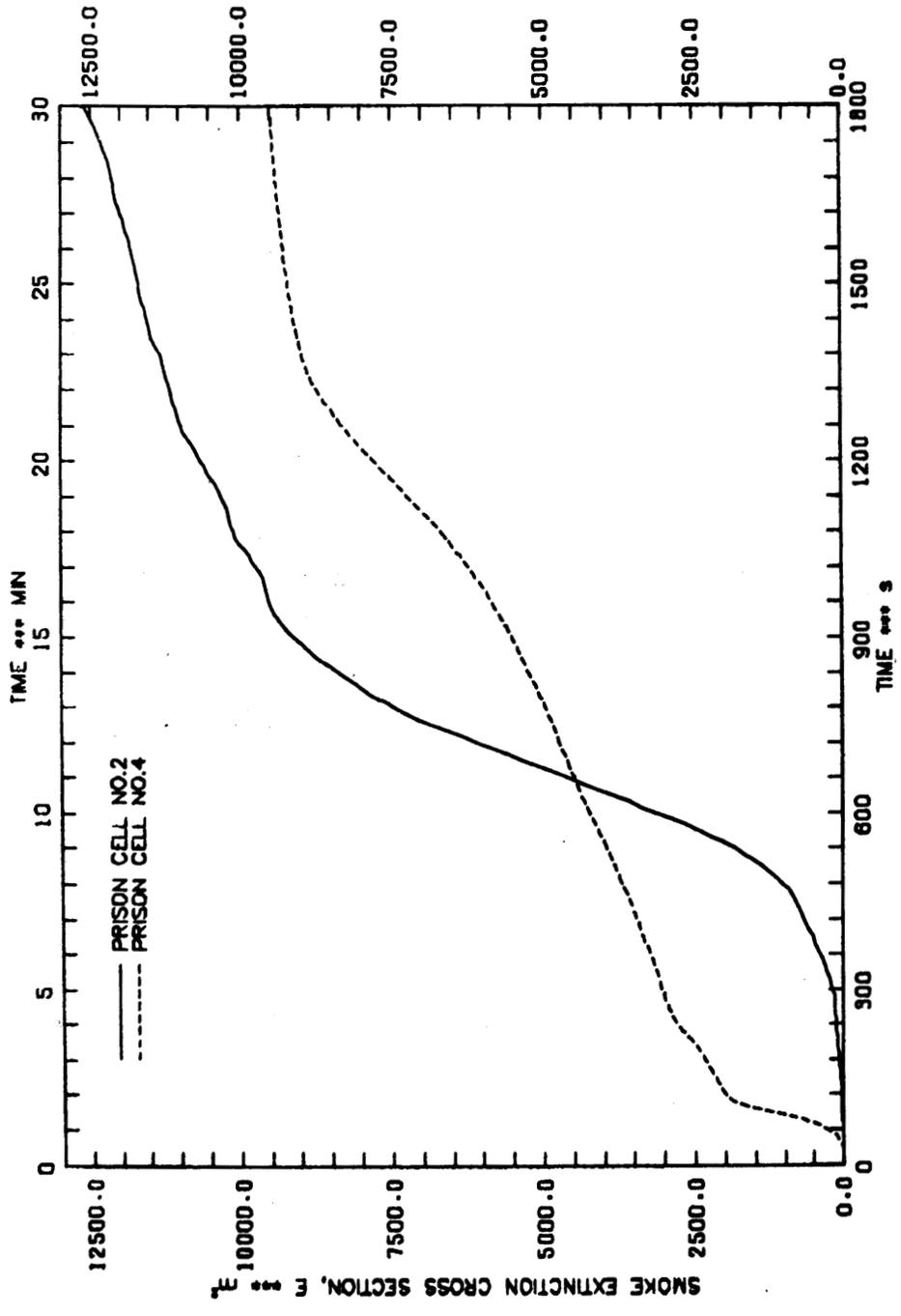
FIGURE 30 - SMOKE EXTINCTION CROSS SECTION VERSUS TIME FOR TESTS 2 AND 4

64
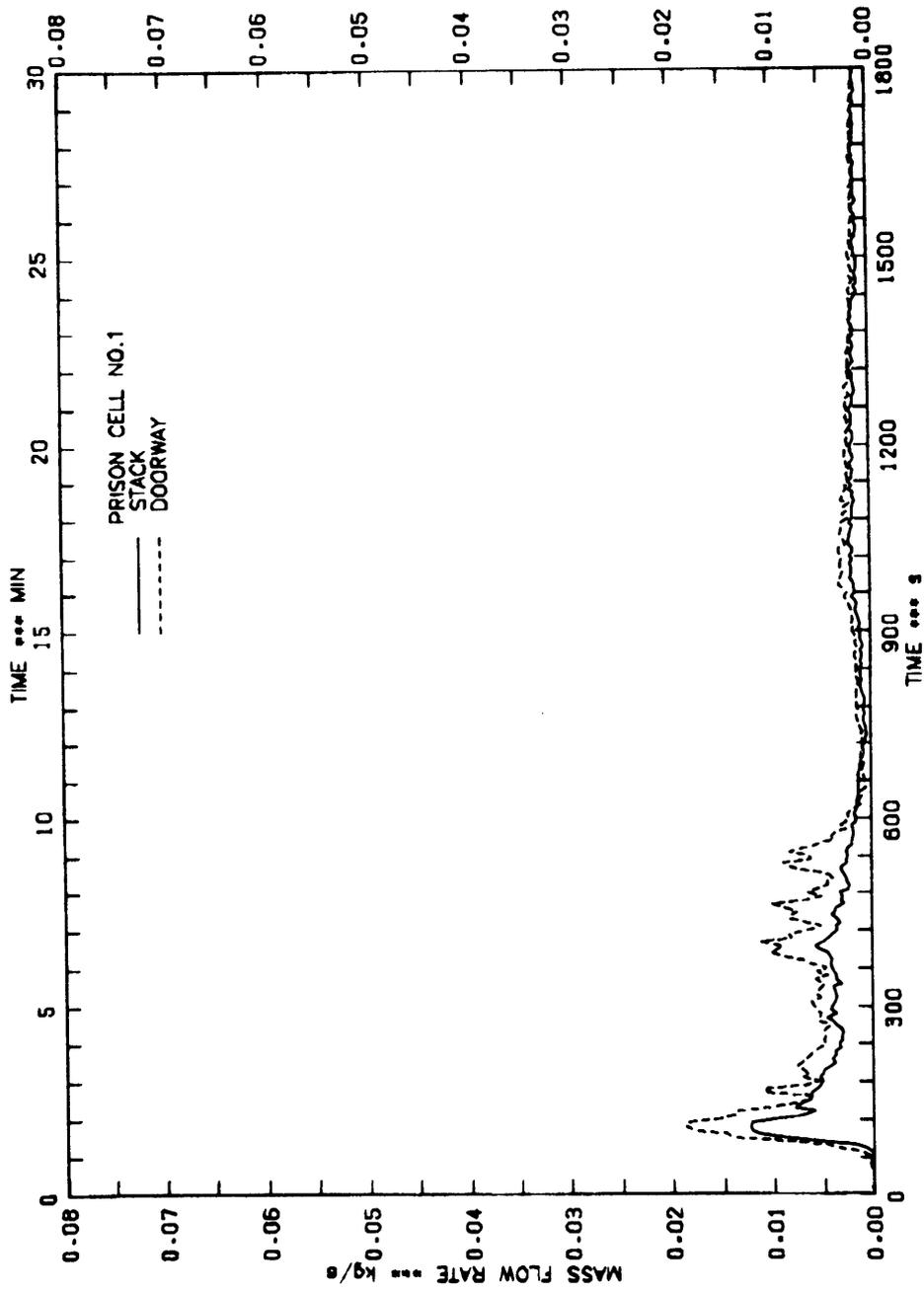
FIGURE 31 — MASS FLOW RATE OF CARBON MONOXIDE VERSUS TIME FOR TEST 1

65
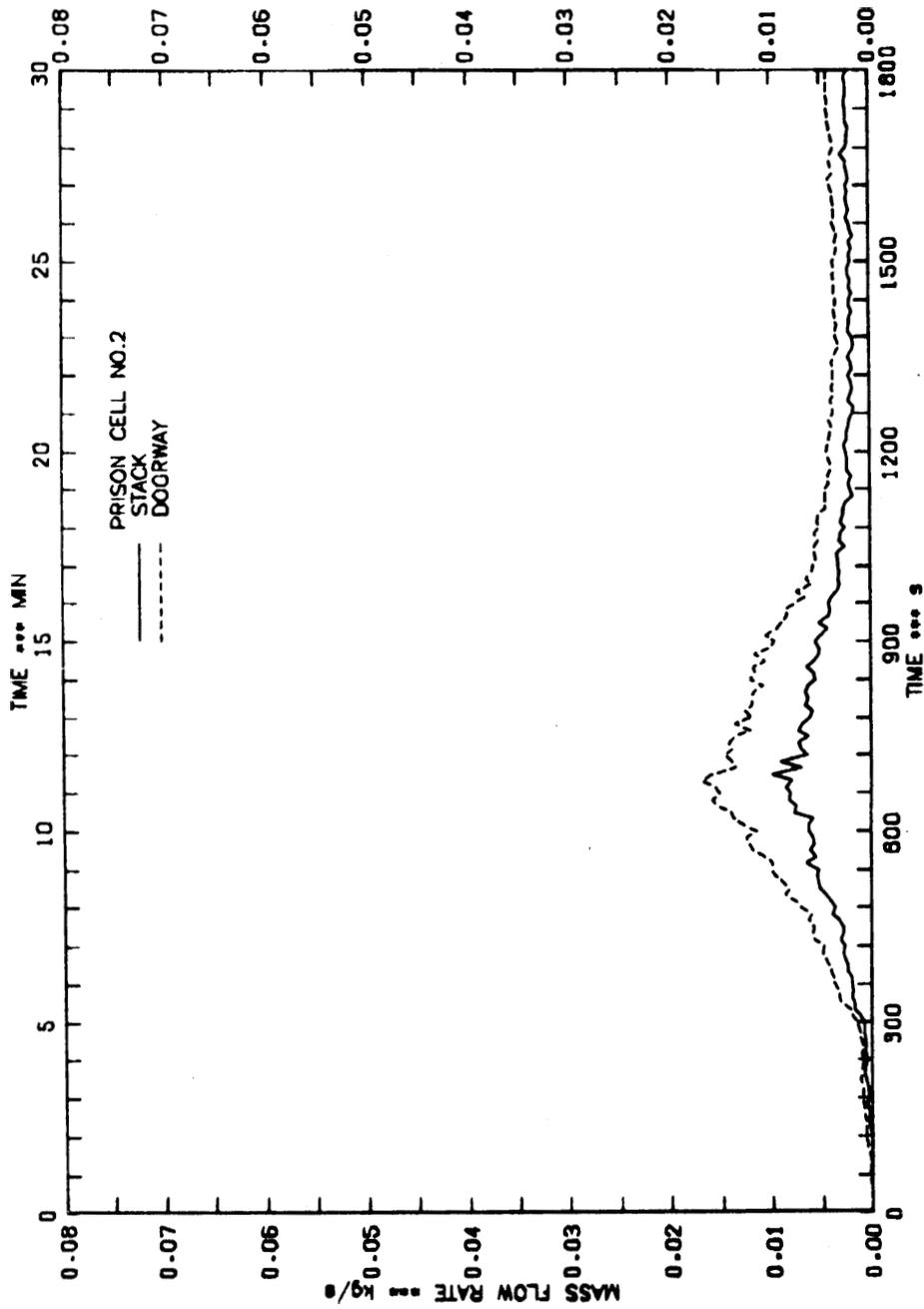
FIGURE 32 – MASS FLOW RATE OF CARBON MONOXIDE VERSUS TIME FOR TEST 2

PRISON CELL NO.2
——— STACK
-------- DOORWAY
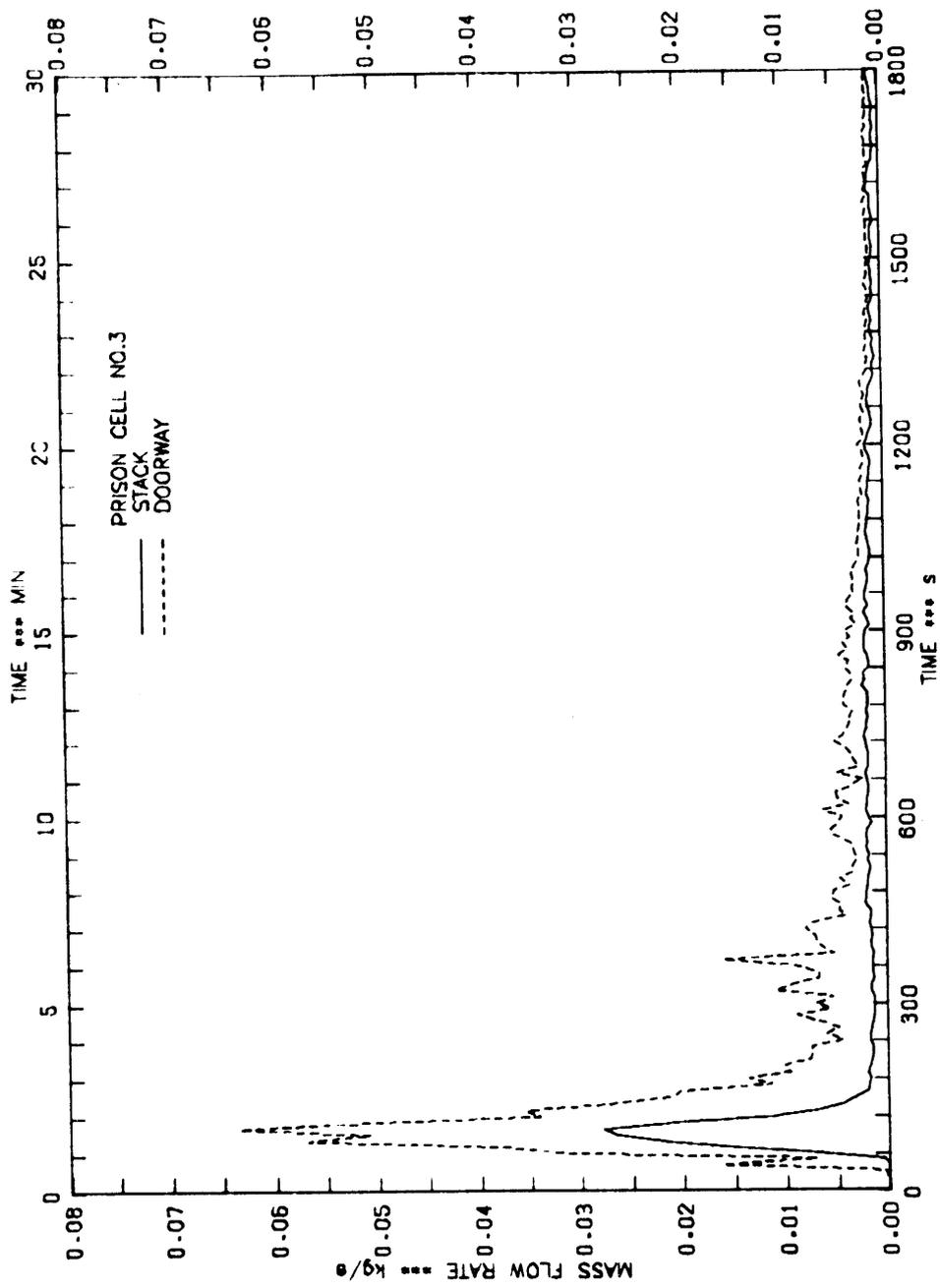
FIGURE 33 – MASS FLOW RATE OF CARBON MONOXIDE VERSUS TIME FOR TEST 3
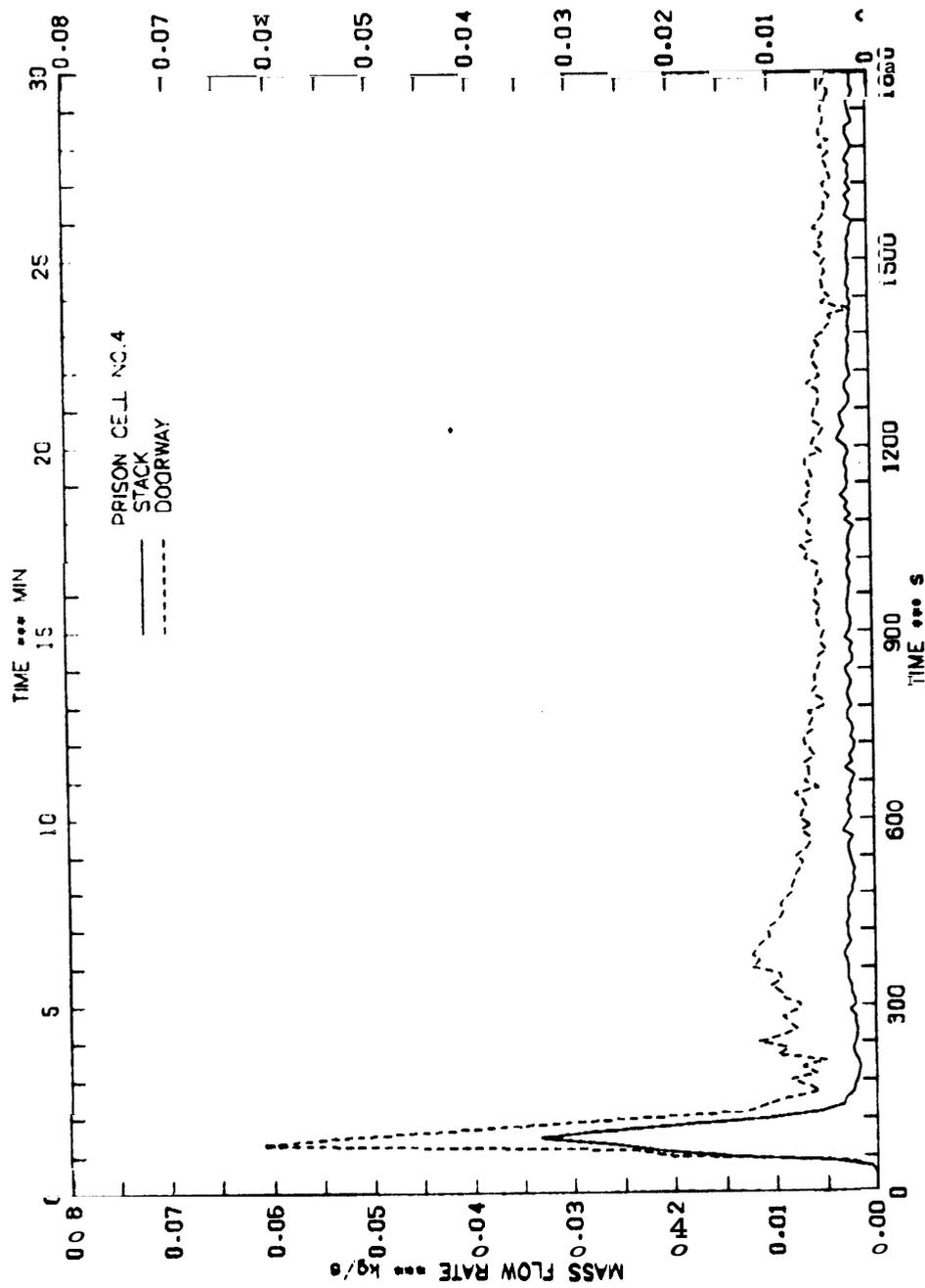
FIGURE 34 — MASS FLOW RATE OF CARBON MONOXIDE VERSUS TIME FOR TEST 4
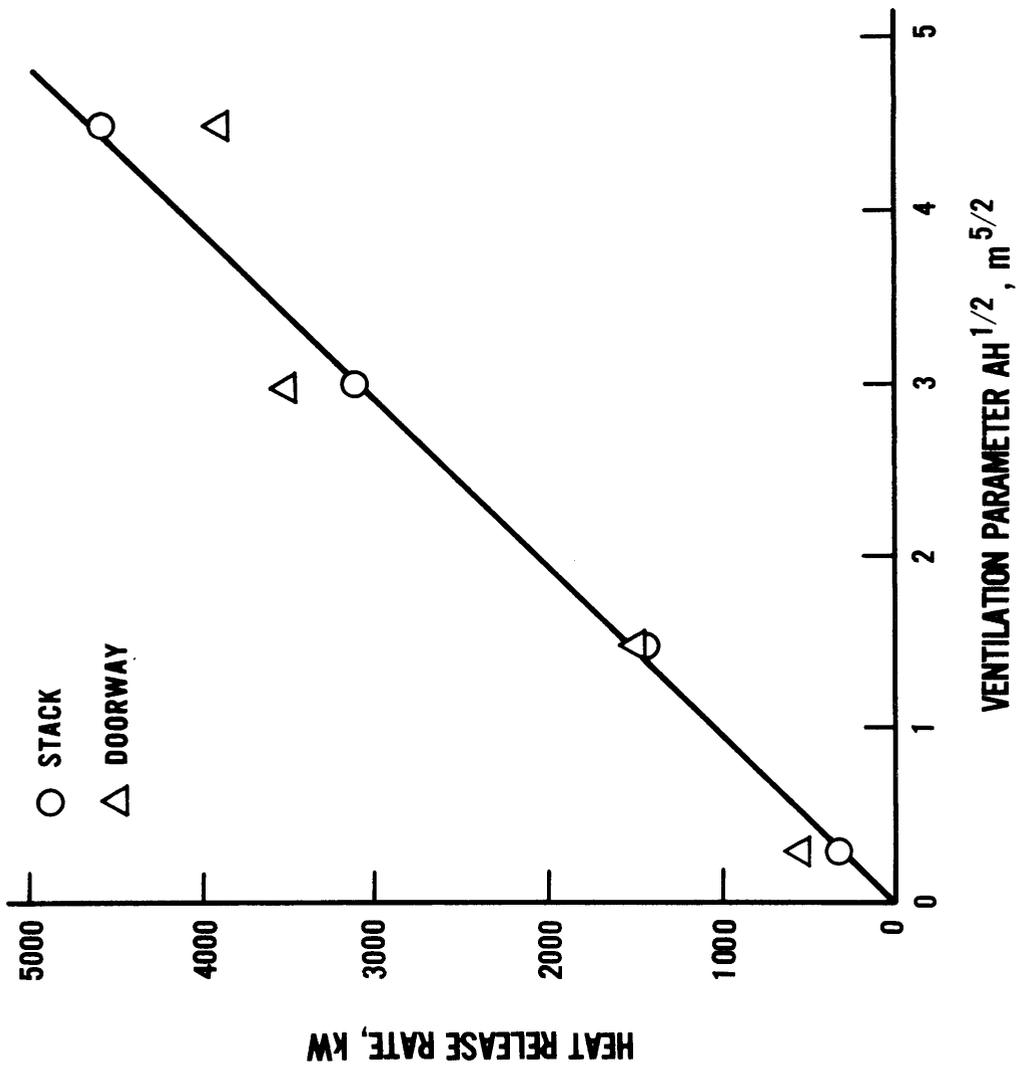
Figure 35. Peak heat release rate vs. doorway ventilation parameter

69

APPENDIX A

A.1 <u>Calculation of Heat Release Rate from Oxygen Depletion Measurement</u>

The formulae given here are taken from a report by Lawson et al.* The rate of heat release from a room fire can be expressed as:

$$\dot{Q} = E X_{O_2}^o \, m\emptyset \, W_{O2}\big/W_{air}$$

where:

$\dot{Q}$ = Rate of heat released from the fire room, MW.

E = Heat per unit mass of oxygen consumed by the burning of materials normally used in the construction and furnishing of rooms, MJ/kg. A value of 13.2 MJ/kg was chosen based on a study by Huggett.**

$X_{O_2}^o$ = Oxygen concentration in ambient air, moles oxygen/moles air.

m = Mass flow rate of air from fire room, kg/s.

W_{O_2} = Molecular weight of oxygen, kg.

W_{air} = Molecular weight of air, kg.

$\emptyset$ = Oxygen depletion of the air.

The oxygen depletion can be further defined as:

_____
*Lawson, J. R. et al, The Development of an Oxygen Consumption Calorimeter, NBSIR in preparation.
Huggett, C., Estimation of Rate of Heat Release by Means of Oxygen Consumption Measurement, Fire and Materials, **4, 61-65, 1980.

$$\phi = \frac{x^o_{O_2} - x^A_{O_2}}{x^o_{O_2}\left(1 - x^A_{O_2}\right)} \quad \text{if the } CO_2 \text{ is trapped ahead of the oxygen analyzer}$$

and

$$\phi = \frac{x^o_{O_2} - x^B_{O_2}/\left(1 - x_{CO_2}\right)}{x^o_{O_2}\left[1 - x^B_{O_2}/\left(1 - x_{CO_2}\right)\right]} \quad \text{when } CO_2 \text{ is not trapped}$$

where

$x^A_{O_2}$ = Measured oxygen concentration with CO_2 trapped out

$x^B_{O_2}$ = Measured oxygen concentration when CO_2 is not trapped

x_{CO_2} = Measured concentration of CO_2

As an example of the use of the above formulae, the following table outlines the calculation of the rate of heat release in the case of the calibration[1] burner operating directly under the stack (refer to section 2.4 for further details).

	Heat Input from Propane Burner (kW)	Flow Rate Through Stack (20°C, 1 atm.) (m³/s)	Ambient O_2 Conc. (%)	Measured O_2 Conc. (%)	Measured CO_2 Conc. (%)	Oxygen Depletion ϕ	Rate of Heat Release Q (kW)
CO_2 Removed	485	2.9	20.90	20.06	–	0.0503	517
	1290	2.7	20.90	18.47	–	0.1426	1365
CO_2 Not Removed	485	2.9	20.90	19.93	0.66	0.0501	515
	1290	2.7	20.90	18.08	1.93	0.1446	1384

Note: A value of 12.75 MJ/kg or 16.96 MJ per m³ of oxygen at 20°C and 1 atm. was-used for propane.   Example:
$Q = (16.96 \text{ MJ/m}^3)(0.209)(2.9 \text{ m}^3/\text{s})(0.0503) = 0.517 \text{ MJ/s or } 517 \text{ kW}$

## A.2 Effective Value of $AH^{1/2}$ for Two Vertically Displaced Small Openings in a Room Fire (by W. J. Parker)
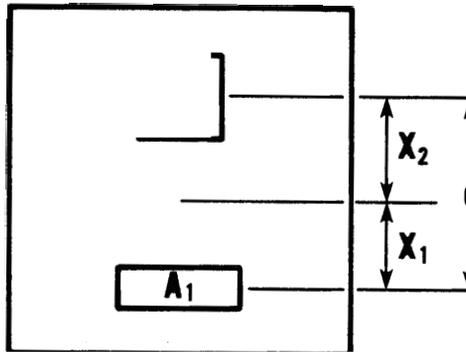
<table>
<tr><td>Figure 1a</td><td>Figure 1b</td></tr>
<tr><td>Room having two opening
areas of A_1 and A_2</td><td>Room having one opening
area of A</td></tr>
</table>
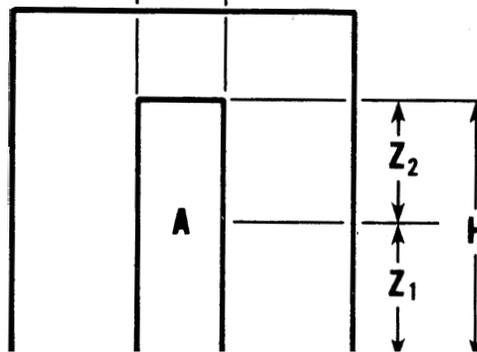
The effective value of the ventilation parameter $AH^{1/2}$ is defined here as the value of $AH^{1/2}$ for a single rectangular opening which would provide the same induced air inflow for a fully developed fire in a room having one opening near the floor and another opening at head level, as shown in Figure 1a. It is assumed that for this case,

(1) there is a uniform temperature, T, in the room and T_o outside the room;

(2) the air flows in through the lower opening and out through the top opening; and,

(3) the height of each opening in Figure la is small enough that the velocity of the air passing through can be considered to be uniform and equal to the value calculated at its center point.

The pressure gradient in the room is given by

$$\frac{dP}{dx} = -\rho_o g \left(1 - \frac{T_o}{T}\right) = \beta$$

where ρ_o is the density of the ambient air; g is the acceleration due to gravity; x_1 and x_2 are the distances from the neutral density plane to the center of the openings in Figure la; and z_1 and z_2 are the distances from the neutral density plane to the bottom and top of the opening in Figure lb, respectively. Then the differential pressure at the center of the openings are βx_1 and βx_2. The corresponding velocities are

$$v_1 = \left(\frac{2\beta x_1}{\rho_o}\right)^{1/2} \qquad \text{and} \qquad v_2 = \left(\frac{2\beta x_2}{\rho}\right)^{1/2}$$

where ρ is the density of the air inside the room. The mass flows are

$$\dot{m}_1 = \rho_o A_1 \left(\frac{2\beta x_1}{\rho_o}\right)^{1/2} \qquad = \qquad \left(2\beta\rho_o x_1\right)^{1/2} A_1$$

and

$$\dot{m}_2 = \rho A_2 \left(\frac{2\beta x_2}{\rho}\right)^{1/2} \qquad = \qquad \left(2\beta\rho x_2\right)^{1/2} A_2 \quad .$$

Since $\dot{m}_1 = \dot{m}_2$ and $x_2 = d - x_1$, the neutral plane height above the center of the lower opening is found to be

$$x_1 = \frac{\left(\frac{\rho}{\rho_o}\right)\left(\frac{A_2}{A_1}\right)^2 d}{1 + \left(\frac{\rho}{\rho_o}\right)\left(\frac{A_2}{A_1}\right)^2}$$

and the mass inflow is given by

$$m_1 = \left(2\beta\rho_o x_1\right)^{1/2} A_1 = \frac{\left(2\beta\rho_o\right)^{1/2}\left(\frac{\rho}{\rho_o}\right)^{1/2} A_2 d^{1/2}}{\left[1 + \left(\frac{\rho}{\rho_o}\right)\left(\frac{A_2}{A_1}\right)^2\right]^{1/2}} \qquad \text{Eq. (1)}$$

For the single doorway case in Figure 1b,

$$\dot{m}_1 = \rho_o W \int_0^{z_1} v\,dz = \rho_o W \int_0^{z_1} \left(\frac{2\beta z}{\rho_o}\right)^{1/2} dz$$

$$\dot{m}_1 = \frac{2}{3}\left(2\beta\rho_o\right)^{1/2} W z_1^{3/2}$$

Similarly,

$$\dot{m}_2 = \frac{2}{3}\left(2\beta\rho\right)^{1/2} W z_2^{3/2} = \frac{2}{3}\left(2\beta\rho\right)^{1/2} W\left(H-z_1\right)^{3/2}$$

The mass balance requires that

$$x_1 = \frac{\left(\frac{\rho}{\rho_o}\right)^{1/3} H}{1 + \left(\frac{\rho}{\rho_o}\right)^{1/3}}$$

so that.

$$m_1 = \frac{\frac{2}{3} \left(2\beta\rho_0\right)^{1/2} WH^{3/2} \left(\frac{\rho}{\rho_0}\right)^{1/2}}{\left[1 + \left(\frac{\rho}{\rho_0}\right)^{1/3}\right]^{3/2}} \qquad\qquad \text{Eq. (2)}$$

The openings shown in Figures 1a and 1b are equivalent if they have the same mass inflow. Comparing equation (1) and (2) and solving for $WH^{3/2} = AH^{1/2}$ we, have the effective value $AH^{1/2*}$ for the room with the two openings. Thus, letting $\frac{\rho}{\rho_0} = \frac{T_0}{T}$, we have

$$AH^{1/2*} = kA_2 d^{1/2}$$

where

$$k = \frac{\frac{3}{2} \left[1 + \left(\frac{T_0}{T}\right)^{1/3}\right]^{3/2}}{\left[1 + \frac{T_0}{T}\left(\frac{A_2}{A_1}\right)^2\right]^{1/2}} .$$

The air temperature in the room in test 2, aside from that near the floor, averaged about 425°C at times between 690 and 770 **s,** at which times the peak rate of heat release occurred at the stack and cell opening, respectively. Then,

$T_0 = 300 \text{ K}$

$T = 698 \text{ K}$

$A_2 = 0.093 \text{ m}^2$

$A_1 = 0.073 \text{ m}^2$

$d = 1.47 \text{ m}$

Hence, $k = 2.67$ and $AH^{1/2*} = 0.30 \text{ m}^{5/2}$ for test 2 with the two openings.

U.S. DEPT. OF COMM. BIBLIOGRAPHIC DATA SHEET *(See instructions)*	1. PUBLICATION OR REPORT NO. NBSIR 82-2469	2. Performing Organ. Report No.	3. Publication Date March 1982

5. AUTHOR(S)

B. T. Lee

6. PERFORMING ORGANIZATION *(If joint or other than NBS, see instructions)* NATIONAL BUREAU OF STANDARDS DEPARTMENTOFCOMMERCE WASHINGTON, D.C. 20234	7. Contract/Grant No.
	8. Type of Report & Period Covered

9. SPONSORING ORGANIZATION NAME AND COMPLETE ADDRESS *(Street, City. State, ZIP)*

Sponsored in part by: National Institute of Justice
U. S. Department of Justice
Washington, DC

10. SUPPLEMENTARY NOTES

☐ Document describes a computer program; SF-185, FIPS Software Summary, is attached.

11. ABSTRACT *(A 200-word or less factual summary of most significant information. If document includes a significant bibliography or literature survey, mention it here)*

The rates of heat release and smoke development from a fire in a typical prison cell configuration were examined under four doorway ventilation conditions, Peak heat release rates varied from about *4500* kW for a *3.34* m^2 doorway opening down to *340* kW for a 0.17 m^2 opening. However, the total and rate of smoke generation were greater with the small opening. The peak carbon monoxide production rate varied from *0.03* kg/s for the large opening to 0.01 kg/s for the smallest opening. The quantity of carbon monoxide generated, however, was highest for the smallest opening with 5.3 kg produced over the fire duration of 1800 s. During the peak fire development in the configuration with the larger openings, temperatures inside the room reached about 1000°C with roughly two-thirds of the heat lost to the cell room boundaries. Peak thermal fluxes inside the room generally exceeded the ignition threshold value of about 20 kW/m^2 for clothing, bedding, and other light combustible fuel for all of the tests.

12. KEY WORDS *(Six to twelve entries; alphabetical order; capitalize only proper names; and separate key words by semicolons)*

Fire growth; fuel load; heat release rate; prison cell fire; smoke

13. AVAILABILITY	14. NO. OF PRINTED PAGES
☒ Unlimited ☐ For Official Distribution. Do Not Release to NTIS ☐ Order From Superintendent of Documents, U.S. Government Printing Office, Washington, D.C. 20402.	80
☒ Order From National Technical Information Service (NTIS), Springfield, VA. 22161	15. Price 10.50